



Electrochemically Fabricated Alloys and Semiconductors Containing Indium

Yonghwa Chung and Chi-Woo Lee[†]

Department of Advanced Materials Chemistry, Korea University, 2511 Sejongro, Sejong 339-700, Republic of Korea

ABSTRACT :

Although indium (In) is not an abundant element, the use of indium is expected to grow, especially as applied to copper-indium-(gallium)-selenide (CI(G)S) solar cells. In future when CIGS solar cells will be used extensively, the available amount of indium could be a limiting factor, unless a synthetic technique of efficiently utilizing the element is developed. Current vacuum techniques inherently produce a significant loss of In during the synthetic process, while electrodeposition exploits nearly 100% of the In, with little loss of the material. Thus, an electrochemical process will be the method of choice to produce alloys of In once the proper conditions are designed. In this review, we examine the electrochemical processes of electrodeposition in the synthesis of indium alloys. We focus on the conditions under which alloys are electrodeposited and on the factors that can affect the composition or properties of alloys. The knowledge is to facilitate the development of electrochemical means of efficiently using this relatively rare element to synthesize valuable materials, for applications such as solar cells and light-emitting devices.

Keywords: Indium, Alloy, Semiconductor, Electrodeposition

Received June 16, 2012 : Accepted August 2, 2012

1. Introduction

Indium is a rare metal, and its concentration in the earth's crust is about 0.1 parts per million. Indium cannot be used as a structural metal due to its mechanical properties, but it is used for the production of alloys and semiconductors¹⁾. The physical, chemical, and electrochemical properties and behaviors of indium have been investigated in a number published reports,¹⁻⁶⁾ including our recent work.⁷⁾ The addition of indium improves the strength, hardness, corrosion resistance, and wettability of an alloy. Alloys containing indium are used as low-melting materials, glass-sealing materials, and dental materials, among other uses.⁸⁾ Semiconductors containing indium are used in infrared detectors, magnetoresistors, optoelectronic

materials, absorber materials for solar cells, etc.⁹⁻²⁰⁾ The current major application of indium is in the formation of transparent conducting materials (ITO, tin-doped indium oxide).²¹⁾ In this review, we may use the term "alloys" to refer to both alloys and semiconducting materials.

Alloys containing indium can be classified as binary (AgIn, InBi, InP, InSe, etc.), ternary (GaInSb, CuInSe, etc.), quaternary (CuInGaSe (CIGS), CuInSSe, etc.), and quinary (CdGeSnZnIn, etc.) alloys.^{1,2)} The current interest in indium is associated with chalcopyrite solar cells and CIGS solar cells in particular, that contain the element, due to their high efficiency and long-term stability.²⁰⁾ In future when CIGS solar cells will be extensively used, the available amount of indium will be a limiting factor for the proliferation of the thin-film solar cells, unless effective techniques, such as an electrodeposition, that are alternatives to vacuum techniques are fully developed to utilize the element.

[†]Corresponding author. Tel.: +82-44-860-1333
E-mail address: cwlee@korea.ac.kr

Thin films of alloys can be prepared using physical or chemical methods. Physical methods include thermal evaporation,^{22,23)} sputtering,^{24,25)} and pulsed laser deposition.²⁶⁾ Chemical methods for the preparation of thin film alloys include approaches such as chemical vapor deposition,^{27,28)} chemical bath deposition,²⁹⁾ electrodeposition,^{8,29)} and spray pyrolysis.^{30,31)} Molecular-beam epitaxy (MBE)^{32,33)} can be a physical or a chemical method, because the beam of materials can be generated by physical means or by chemical reactions. Among the methods used to grow thin alloy films of indium, an electrochemical approach may be superior, because unlike the other methods, it enables up to 98% of the material to be effectively used.²⁹⁾

Cathodic deposition of different elements for the formation of alloys from aqueous electrolytes is a process that has been known for a long time.^{29,34)} When electrodeposition is performed in aqueous solutions, it may be simpler and cost less than thermal deposition. The electrodeposition of an alloy is carried out through the codeposition or sequential deposition of two or more elementary ion species.^{9,20,35)}

For the preparation of thin film alloys by electrodeposition, a number of variables must be considered, such as the electrolyte, the electrodes, the applied potential or current, and the additive used. The electrolyte or bath consists of the ions to be electrodeposited. Metal ions are deposited on the cathode from the aqueous solution, and the counter-ion (mostly anion) in the solution is also important for its interaction or its ability to form a complex with a metal ion. Depending on the purpose of the alloy film, a suitable electrode substrate on which the electrodeposition takes place must be determined. Electrical energy can be supplied through direct current at a constant potential, direct current at a constant current, or a current or potential waveform or pulse. An additive is sometimes included in the bath to bring closer the deposition potentials of individual elements or to improve the quality of the electrodeposits. In most cases of alloy preparation by electrodeposition, post-deposition treatment might be considered. Heat treatment, as a post-deposition treatment, is performed in a vacuum, under inert gas, or in elementary vapors.⁹⁾

In the preparation of alloys, the first thing to consider is the definite ratio of the component elements in the alloy. It is known that the factors that determine the possibility of joint electrochemical deposition of two or more elements at a certain ratio in an alloy are the

following: the equilibrium potentials of the metals and nonmetallic compounds, their polarizations during the discharge of the corresponding ions at the cathode from a given electrolyte, the concentration ratio of metal ions and nonmetallic anions being deposited in the electrolyte, their ability to form complex compounds, the presence of surfactants in the electrolyte, overvoltage of the hydrogen evolution during deposition of the alloy, the electrolysis conditions (temperature, current density, pH of the solution, deposition time, stirring), etc.³⁶⁾

In this work, we review electrochemically fabricated alloys and semiconductors that contain indium in an aqueous solution, with a particular focus on the conditions under which alloys are electrodeposited and on the factors that can affect the composition or properties of alloys. Our aim is to assist in the discovery of ways to use this relatively rare element efficiently. The most recent review on the subject was published in 1981,⁸⁾ and here, we provide an update on this topic.

2. Preparation

2.1. Potentiostatic deposition

The electrodeposition of alloys can take place through either the codeposition (one-step) or sequential (multi-step) deposition of the individual components in the alloys. In any case, prior to electrodeposition, the standard electrode potential of each ion involved in the electrochemical processes must be considered. In the codeposition of alloys, the ratio of components depends on the applied potential. The standard reduction potentials of the elements included in alloys that is reviewed here are listed in Table 1.³⁷⁾

The codeposition of metal alloys can be carried out from a solution containing component ions at the deposition potential of the less noble component. However, interactions between the components in the deposition usually shift the deposition potential of the alloy to those values that are positive relative to the deposition potential of the less noble component.³⁴⁾ In some cases, e.g., for Ni and Sn alloys, the deposition potential is positive even relative to that of the noble component.³⁸⁾ Because nonmetals such as S and Se, and semimetals such as As, Sb, and Te can be deposited cathodically from solutions of complex ions or molecules, cathodic codeposition of one of these elements and of metallic elements may also be possi-

Table 1. Standard reduction potentials of elements included in the In-alloys treated in this review

Reaction	E°/V vs. SHE
$\text{In}^{3+} + 3e \rightleftharpoons \text{In}$	-0.3382
$\text{In}^{3+} + 2e \rightleftharpoons \text{In}^+$	-0.443
$\text{In}^+ + e \rightleftharpoons \text{In}$	-0.14
$\text{Ag}^+ + e \rightleftharpoons \text{Ag}$	0.7996
$\text{As} + 3\text{H}^+ + 3e \rightleftharpoons \text{AsH}_3$	-0.608
$\text{HAsO}_2 + 3\text{H}^+ + 3e \rightleftharpoons \text{As} + 2\text{H}_2\text{O}$	0.248
$\text{AsO}_2^- + 2\text{H}_2\text{O} + 3e \rightleftharpoons \text{As} + 4\text{OH}^-$	-0.68
$\text{Bi}^{3+} + 3e \rightleftharpoons \text{Bi}$	0.308
$\text{Cu}^{2+} + 2e \rightleftharpoons \text{Cu}$	0.3419
$\text{Cu}^{2+} + e \rightleftharpoons \text{Cu}^+$	0.153
$\text{Cu}^+ + e \rightleftharpoons \text{Cu}$	0.521
$\text{Cd}^{2+} + 2e \rightleftharpoons \text{Cd}$	-0.4030
$\text{Ni}^{2+} + 2e \rightleftharpoons \text{Ni}$	-0.72
$\text{Pb}^{2+} + 2e \rightleftharpoons \text{Pb}$	-0.1262
$\text{Pd}^{2+} + 2e \rightleftharpoons \text{Pd}$	0.951
$\text{Sb} + 3\text{H}^+ + 3e \rightleftharpoons \text{SbH}_3$	-0.510
$\text{Sb}_2\text{O}_3 + 6\text{H}^+ + 6e \rightleftharpoons 2\text{Sb} + 3\text{H}_2\text{O}$	0.152
$\text{Se} + 2e \rightleftharpoons \text{Se}^{2-}$	-0.924
$\text{Se} + 2\text{H}^+ + 2e \rightleftharpoons \text{H}_2\text{Se}(\text{aq})$	-0.082
$\text{H}_2\text{SeO}_3 + 4\text{H}^+ + 4e \rightleftharpoons \text{Se} + 3\text{H}_2\text{O}$	0.74
$\text{SeO}_3^{2-} + 3\text{H}_2\text{O} + 4e \rightleftharpoons \text{Se} + 6\text{OH}^-$	-0.366
$\text{Sn}^{2+} + 2e \rightleftharpoons \text{Sn}$	-0.1375
$\text{Te} + 2e \rightleftharpoons \text{Te}^{2-}$	-1.143
$\text{TeO}_2 + 4\text{H}^+ + 4e \rightleftharpoons \text{Te} + 2\text{H}_2\text{O}$	0.593
$\text{Tl}^{3+} + 3e \rightleftharpoons \text{Tl}$	0.741
$\text{Zn}^{2+} + 2e \rightleftharpoons \text{Zn}$	-0.7618

ble.^{29,39-41}) In the electrodeposition of an alloy in which one elementary component is much nobler than the other, a complexing agent must be added in order to equalize the deposition potentials. Acetate, citrate, tartrate, cyanide, EDTA (ethylenediamine tetraacetic acid), triethanolamine, and CTAB (cetyltrimethylammonium bromide) are used as complexing agents.⁸⁾

2.1.1. One-step deposition

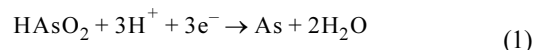
One-step deposition is to prepare alloy films by simultaneous electrodeposition of constituent elements in solutions containing all the components of the alloy. In order to choose the constant deposition potential, a number of factors such as the standard

reduction potentials of component ions, the interaction between the components, the hydrogen evolution, and the polarization characteristics of the bath have to be considered.⁹⁾

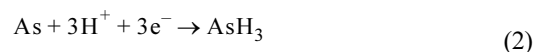
2.1.1.1. Binary alloys

Saidman *et al.* studied the electrodeposition of In and of Zn on aluminum⁴³⁾ and vitreous carbon⁴⁴⁾ under potentiostatic conditions. They investigated the effects of the substrate and of agitation on the electrodeposition of In and of Zn. For the deposition on Al at -1.5 V vs. SCE for 10 min without agitation, indium-rich deposits were obtained, while with agitation, Zn-rich deposits were obtained. They concluded that the deposition of indium on freshly nucleated Zn was favored at a high cathodic potential without agitation, which indicated the Zn catalytic effect. When deposition was carried out on vitreous carbon at -1.2 V vs. SCE for 10 min under stagnant conditions, the deposition of indium hydroxide was favored, due to the localized alkalization by the hydrogen evolution reaction, and deposits with the same atomic percentage of In and Zn were attained. However, processes involving the codeposition of Zn and In on both Al and vitreous carbon occurred without the formation of alloys or intermetallic compounds, by the interaction of Zn and In.

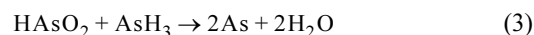
Ortega and Herrero⁴¹⁾ studied the electrodeposition of InAs thin films from solutions containing 0.02 M AsCl_3 , 0.02 M InCl_3 , and 0.3 M citric acid at -1.40 V vs. SCE. They reported that arsenic was formed from the chemical interaction between the AsH_3 formed on the cathode and the HAsO_2 contained in the solution, as follows:



$$E^{\circ} = 0.248 \text{ V vs. SHE}$$



$$E^{\circ} = -0.608 \text{ V vs. SHE}$$



During the electrodeposition of the InAs layers, photoelectrochemical activity was observed, and the InAs layers prepared in this study displayed low crystallinity.

Dalchiale *et al.* performed the codeposition of InAs alloy films from an acidic solution with a pH of 2 containing NaAsO_2 , $\text{In}_2(\text{SO}_4)_3$, potassium citrate, and

K_2SO_4 at a constant potential that ranged from -0.800 to -1.250 V vs. SCE.⁴⁵⁾ The indium content of the deposited film depended on the applied potential and the indium concentration of the bath solution.

InSb thin films were prepared by electrodeposition from a bath containing $SbCl_3$, $InCl_3$, and citric acid^{41,46)} or a bath of $SbCl_3$, $InCl_3$, citric acid, and citrate.^{47,48)} Electrodepositions of InSb were carried out at potentials of -0.65 to -1.55 V vs. SCE and at room temperature. Ortega and Herrero⁴¹⁾ obtained the polycrystalline fcc InSb that was free of In and Sb phases at -0.85 V vs. SCE. McChesney *et al.*⁴⁶⁾ reported that InSb electrodeposits (-0.6 to -1.2 V vs. Ag/AgCl) were grown that had an excess of either In (at -1.2 V) or Sb (at -0.6 V), and that mixtures of In, Sb, and InSb grown on Ti substrates indicated the presence of kinetic barriers to the formation of InSb. Fulop *et al.*⁴⁷⁾ prepared polycrystalline InSb films with thicknesses in the micron range at a potential of -1.2 V vs. Ag/AgCl. A molar ratio of In^{3+} to Sb^{3+} of 1.5 ± 0.1 in the electrolyte yielded a deposit with an atomic ratio of In to Sb of 1.0 ± 0.1 . Khan *et al.*⁴⁸⁾ reported the fabrication of InSb nanowire arrays with diameters of 200 nm and 30 nm by electrodeposition at -1.5 V vs. Ag/AgCl inside the nanochannels of Au-sputtered anodic alumina membranes (AAM).

InSe thin films were deposited from acidic aqueous solutions containing In^{3+} and SeO_2 (or H_2SeO_3) at potentials that ranged from -0.8 to -1.35 V vs. SCE⁴⁹⁻⁵⁵⁾. The indium ions were from chloride^{49,50,54,55)} or sulfate⁵¹⁻⁵³⁾ salts. In the deposition of InSe, the pH of the bath solution was below 1.7,^{49,50,52,54,55)} 2.4,⁵³⁾ or 3.45.⁵¹⁾ Kampmann *et al.*⁵³⁾ performed the electrodeposition of

InSe on an ITO substrate at -1.1 V vs. MSE and at $80^\circ C$. Massaccesi *et al.*⁵¹⁾ prepared In_2Se_3 films on tin oxide substrates at $22^\circ C$ and $82^\circ C$. Using XRD measurement, they observed that In_2Se_3 films prepared at $82^\circ C$ had a better crystallinity than those obtained at $22^\circ C$.

In most cases, CuIn alloys were prepared for the fabrication of $CuInS(Se)_2$ during the study of its application to solar cells. CuIn layers were deposited from a solution of Cu^{2+} (or Cu^+) and In^{3+} at a potential that ranged from -0.65 to -1.2 V vs. SCE.^{56-59,97)} Metal ions were introduced as sulfate salts^{56,57,97)} or chloride salts.^{58,59)} The pH of the bath solution was 2-3.5. Nakamura⁵⁹⁾ reported that the morphology of the electrodeposited CuIn was improved by using a solution with a pH of 3.22 without adding HCl. Pottier and Maurin⁵⁷⁾ obtained a powdery mixture of $Cu + Cu_4In + Cu_9In_4$ beyond $E = -1.06$ V vs. SSE, and well-crystallized layers of Cu_9In_4 beyond -1.4 V vs. SSE. Prosin *et al.*⁵⁸⁾ prepared CuIn alloys by electrodepositing them under a diffusion-limited current (at a potential of -0.825 V vs. Ag/AgCl). Because the limiting current for the diffusion of the copper ions was not affected by the simultaneous deposition of indium ions, copper and indium were codeposited onto the electrode surface. The $[Cu]/[In]$ ratio in the films showed a linear correlation with the $[Cu]/[In]$ ratio in the solution. Ribeaucourt *et al.*⁹⁷⁾ prepared CuIn films from a solution of Cu^{2+} , In^{3+} , and citrate, with a pH of 2 at a potential of -1.6 V vs. MSE for 45 min. They reported that the CuIn electrodeposition proceeded predominantly through the formation of binary phases, such as Cu_2In and CuIn, and that the CuIn deposit was

Table 2. Preparation conditions of CuInSe by potentiostatic one-step deposition

Electrolytes	pH and temp. of solutions	Complexants	Applied potential (V vs. SCE)	References
Cu^+ , In^{3+} , Se^{4+} , Cl^-	1, r.t.	Triethanolamine	-0.7 to -1.0	29, 60
Cu^+ , In^{3+} , Se^{4+} , Cl^-	4.5	SCN^-	-0.8	61
$CuCl$, $In_2(SO_4)_3$, Se^{4+}	5, $25^\circ C$	SCN^-	-0.7	62
$CuSO_4$, $In(SO_3NH_2)_3$, Se^{4+}	1.7, r.t.	-	-0.56 to -0.76	63
Cu^{2+} , In^{3+} , Se^{4+} , SO_4^{2-}	≤ 2.45	-	-0.5 to -0.75	52, 84, 91, 153
Cu^{2+} , In^{3+} , Se^{4+} , SO_4^{2-}	1, $50-55^\circ C$	-	-0.8	64
Cu^{2+} , In^{3+} , Se^{4+} , SO_4^{2-}	≤ 3.3 , $\leq 37^\circ C$	Citrate	-0.4 to -0.8	57, 65-69, 80-83, 88, 90
Cu^{2+} , In^{3+} , Se^{4+} , Cl^-	1.5, $24^\circ C$	-	-0.4 to -0.9	70, 78, 79, 86
Cu^{2+} , In^{3+} , Se^{4+} , Cl^-	2	EDTA	-0.45 to -0.75	85
Cu^{2+} , In^{3+} , Se^{4+} , Cl^-		Citrate	-0.29 to -0.65	87
Cu^{2+} , In^{3+} , Se^{4+} , NO_3^-	8.5	Diethylenetriamine	-1.15	89

not dense and was dendritic. They detected the presence of a small amount of indium oxide or indium hydroxide by means of EDS analysis.

2.1.1.2. Ternary and quaternary alloys

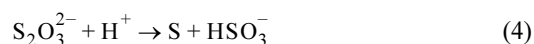
The codeposition of the absorber layers in photovoltaic cells, which are composed of materials such as CuInSe(S, Te)₂ and Cu(InGa)Se₂, have been studied by many authors in order to obtain thin films with the best optoelectronic properties. The influence of film deposition parameters such as the bath composition, pH, deposition potential, deposition time, bath temperature, and material purity on the film properties have been studied.

Bhattacharya prepared CuInSe₂ (CIS) thin films under potentiostatic conditions on F-doped SnO₂ coated glass.²⁹⁾ The plating solution was prepared from 0.018 M InCl₃, 0.018 M CuCl, 0.025 M SeO₂, 0.006% (v/v) triethanolamine, and 0.007% (v/v) ammonia solution. The deposition was carried out at -700 mV vs. SCE, at a pH of 1, at room temperature with stirring. Following Bhattacharya's report, codepositions of CIS were carried out from solutions of Cu⁺, In³⁺, and Se⁴⁺ or from solutions of Cu²⁺, In³⁺, and Se⁴⁺; SeO₂ or H₂SeO₃ was used as the Se source. The preparation conditions used in studies of the potentiostatic codeposition of CIS are summarized in Table 2.

A CuInSe₂-based p-n junction was deposited from a single aqueous solution using a step function potential by Raffaele *et al.*¹¹³⁾ CIS film was grown on an ITO glass substrate or a molybdenum substrate in a bath containing CuSO₄, In₂(SO₄)₃, SeO₂, and sodium citrate. A 1.0 mm film was deposited at -1.0 V vs. SCE, after which the potential was immediately changed to -1.3 V vs. SCE prior to depositing a 0.1 mm film on the first CIS film. The films deposited at potentials less negative than -1.2 V vs. SCE seemed to be p-type, and those deposited at more negative potentials seemed to be n-type.

Firstly, CuInS₂ thin films could be electrodeposited in a one-step process without the usual heat treatment

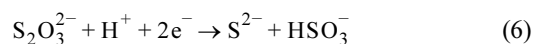
in an H₂S atmosphere. In the codeposition of CuInS₂ thin films, thiourea or sodium thiosulfate (Na₂S₂O₃) was used as the sulfur source.^{40,56,92,93)} In the electrodeposition of Cu₂S from an acidic solution containing CuSO₄ and Na₂S₂O₃,⁹⁴⁾ thiosulfate ions worked not only as the source of sulfur but also as a reducing agent. When the pH is below around 4.4, the decomposition of S₂O₃²⁻ ions is known to form S and HSO₃⁻ through the following reaction:



where S is colloidal sulfur. The colloidal sulfur is consumed to form sulfide through the subsequent electrochemical reaction:



The total reaction is as follows:



In this study, Cu₂S was formed because Na₂S₂O₃, functioning as a reducing agent, reduced the Cu²⁺ ion to Cu⁺ ion.

A deposited CuInS₂ film produced from a solution of S₂O₃²⁻ was found to have a sufficiently high sulfur content as compared to a film deposited using thiourea as the sulfur source.⁹³⁾ The film deposited using Na₂S₂O₃ was also found to have an excellent morphology as compared with the electrodeposited Cu-In precursors with a waste thread-like morphology that did not change after annealing in an H₂S flow. The pH of the solutions was less than 3 in both cases. Table 3 lists the conditions for CuInS₂ codeposition.

Bhattacharya *et al.* prepared CuInTe₂ thin films under potentiostatic conditions from a plating solution containing InCl₃, CuCl, TeO₂, triethanolamine, and ammonia. The deposition was carried out at -1.0 V vs. SCE, at a pH of 1, at room temperature under constant stirring.⁶⁰⁾ Ishizaki *et al.*⁹⁵⁾ obtained the best CuInTe₂ film from a solution with a pH of 1 containing 0.25

Table 3. Preparation conditions for CuInS₂ by potentiostatic one-step deposition

Electrolytes	S source	pH and temp. of solutions	Complexants	Applied potential (V vs. SCE)	References
Cu ⁺ , In ³⁺ , Cl ⁻	Thiourea	2	Triethanolamine	-1.5 to -2.0	40, 56
Cu ²⁺ , In ³⁺ , SO ₄ ²⁻	Na ₂ S ₂ O ₃	1.5	-	-0.95	92
Cu ²⁺ , In ³⁺ , Cl ⁻	Thiourea and Na ₂ S ₂ O ₃	2-2.5, 20-70°C	-	-0.85	93

Table 4. Preparation conditions for CIGS by potentiostatic one-step deposition

Electrolytes	pH and temp. of solutions	Complexants	Applied potential	References
$\text{Cu}^{2+}, \text{In}^{3+}, \text{Ga}^{3+}, \text{Se}^{4+}, \text{Cl}^-$	24°C	-	-1.0 V vs. Pt ref.	98-101
$\text{Cu}^{2+}, \text{In}^{3+}, \text{Ga}^{3+}, \text{Se}^{4+}, \text{Cl}^-$	$\leq 2.11, 24^\circ\text{C}$	-	-0.6 to -0.7 V vs. SCE	79, 102, 103
$\text{Cu}^{2+}, \text{In}^{3+}, \text{Ga}^{3+}, \text{Se}^{4+}, \text{Cl}^-$	2.4	Sulfamate	-0.6 V vs. SCE	104
$\text{Cu}^{2+}, \text{In}^{3+}, \text{Ga}^{3+}, \text{Se}^{4+}, \text{SO}_4^{2-}$		Citric acid	-0.5 to -0.7 V vs. SCE	90
$\text{Cu}^{2+}, \text{In}^{3+}, \text{Ga}^{3+}, \text{Se}^{4+}, \text{SO}_4^{2-}$	1.6-2.6, r.t.	-	-0.61 to -1.05 V vs. NHE	105

mM CuCl_2 , 10 mM InCl_3 , and 0.50 mM TeO_2 in a deposition potential ranging from -0.660 V to -0.500 V vs. Ag/AgCl , and at 363 K. This film had a band gap of 0.98 eV.

Mengoli *et al.* prepared $\text{InAs}_{1-x}\text{Sb}_x$ using potentiostatic codeposition.⁹⁶⁾ $\text{InAs}_{1-x}\text{Sb}_x$ alloy was obtained from a solution containing SbCl_3 , As_2O_3 , InCl_2 , and citric acid that was deposited onto a nickel-plated copper substrate at -1.0 V vs. SCE.

The codeposition of CuInGa on a Mo-coated glass substrate was carried out in a solution of CuSO_4 , $\text{Ga}_2(\text{SO}_4)_3$, $\text{In}_2(\text{SO}_4)_3$ at a pH of 2.15, at a potential of -1.6 V vs. MSE for 45 min. Sodium citrate was sometimes added.⁹⁷⁾

Thin films of another photovoltaic material, CIGS, were deposited potentiostatically, as listed in Table 4. SeO_2 or H_2SeO_3 was used as the source of selenium.

Diaz *et al.* produced CuInSeTe thin films by electrodeposition onto Mo-coated glass substrates and ITO glass substrates.¹⁰⁶⁾ The composition of the bath solution consisted of aqueous solutions of CuSO_4 , InCl_3 , H_2SeO_3 , TeCl_4 , and 0.5 M citric acid. The best condition for a near stoichiometric composition was a constant deposition potential of -0.5 V vs. SCE for a time greater than 4000 s. The electrodeposited samples were amorphous; however, samples changed to the crystalline quaternary phases by annealing in a Te atmosphere.

2.1.2. Multi-step deposition

Multi-step deposition, which involves sequential depositions of constituent elements in the alloy, can be employed for the preparation of metal alloy. In most cases, a multi-layered alloy film needs thermal treatment to improve its morphology or physical properties.

2.1.2.1. Binary alloys

Depositions of InAs ⁹⁶⁾ and InSb ^{107,108)} performed by sequential electrodeposition have been reported. The

electrodeposition of indium was performed onto electrodeposited arsenic or antimony layers, because the loss of deposited group V element was severe during the annealing treatment when they constituted the outer layer.

In the preparation of InAs thin films, the arsenic layers were deposited from 5 wt% solutions of As_2O_3 in 7 M HCl at -1.0 V vs. SCE and 50°C. The indium layers were deposited from solutions containing InCl_3 , ethanolamine, and ammonia at -1.0 V vs. SCE, 25°C at a pH of 2. For the synthesis of InSb thin films, antimony was deposited from a solution of SbCl_3 , H_2SO_4 , and HCl at -0.25 V vs. SCE for a time sufficiently long to obtain the desired film thickness.^{107,108)} The indium was deposited on an Sb film from a chloride bath containing InCl_3 with a pH ranging from 1.5 to 2.0 at -0.85 V vs. SCE.

Tacconi and Rajeshwar described the electrosynthesis of In_2S_3 film on a sulfur-modified gold substrate.¹⁰⁹⁾ Their approach was as follows: (a) a polycrystalline gold surface was first modified potentiostatically with a sulfur layer in a sulfide-containing bath, (b) in an indium-ion-containing bath, indium was plated onto a sulfur-modified gold substrate by means of underpotential deposition, thus forming indium sulfide, (c) indium continued to be deposited atop the indium sulfide layer in an indium-ion-containing bath, and (d) the sulfidation of the residual indium metal was performed in a sulfide-containing bath. As a result, they were able to observe the anodic formation of the sulfur layer on the polycrystalline gold surface at potentials more positive than -0.40 V, the initial formation of indium sulfide at approximately -0.75 V vs. $\text{Ag}/\text{AgCl}/3\text{M KCl}$, and catalyzed deposition of metallic indium atop the initial indium sulfide layer at approximately -0.70 V.

Herrero^{68,110)} prepared In_2Se_3 thin films via the electrodeposition of selenium and the successive electrodeposition of indium onto Se deposits. The electrodeposition of selenium was carried out from an

aqueous bath that contained SeO_2 , citric acid, and sodium citrate at a pH of 4, with a deposition potential of -0.8 V vs. SCE. The electrodeposition of Se was carried out at 80°C in order to avoid the formation of non-conducting red amorphous selenium where it is possible to obtain metallic gray-black Se. They performed the electrodeposition of indium over Se deposits from solutions containing InCl_3 , ethanolamine, and NH_3 at a potential of -1.1 V vs. SCE and at a pH of 2.

Stickney *et al.* reported the deposition of InAs and InSb films through ECALE (electrochemical atomic layer epitaxy) at room temperature.^{111,112} ECALE, which is based on surface limited reactions, involves using underpotential deposits to form an individual atomic layer of the elements making up a compound. Different solutions and potentials are used for each element, and they are alternated in a cycle. The cycle is repeated to achieve the desired deposit thickness. The deposition of InAs was performed on a Si(100)/Ti/Au substrate.¹¹¹ An As_2O_3 solution with a pH of 4.8, buffered with sodium acetate; an In_2O_3 solution with a pH of 3.0; and a blank solution with a pH of 3.0 were used for the deposition of InAs. The supporting electrolyte was NaClO_4 . The deposition cycle used was as follows: arsenic deposition at -0.615 V vs. Ag/AgCl for 20 s, a switch to -0.715 V to deposit indium for 20 s, a switch to -0.615 V for arsenic deposition, and so on. InSb thin films were electrodeposited on an Au-coated glass electrode.¹¹² The following solutions were used: an $\text{In}_2(\text{SO}_4)_3$ solution with a pH of 3.0 and an Sb_2O_3 solution with a pH of 5.0. For Sb deposits, initial potentials of between -0.400 and -0.500 V were selected, along with an In potential similar to the In potential that had been used to deposit InAs.¹¹¹ The potentials were shifted negatively each step for the first 25 cycles before the steady state potentials were reached and the contact potential was established. Thus the intricate control of pH and electrolyte was required.

2.1.2.2. Ternary and quaternary alloys

Mengoli *et al.* prepared $\text{InAs}_{1-x}\text{Sb}_x$ thin films⁹⁶ of two-layer (AsSb alloy and In layers) and InGaSb three-layer samples¹⁰⁷ (Ga onto InSb two-layer samples) by sequential electrodeposition. For the deposition of $\text{InAs}_{1-x}\text{Sb}_x$ thin films,⁹⁶ first, AsSb alloys were electrodeposited onto nickel-plated copper sheets from citric acid solutions containing equimolar amounts of As_2O_3 and SbCl_3 at -0.7 V vs. SCE at 25°C . Indium

layers on AsSb layers were deposited in solutions of InCl_3 , ethanolamine, and NH_3 with a pH of 12, at -1.0 V vs. SCE at 25°C .

In the preparation of $\text{InAs}_{1-x}\text{Sb}_x$ thin films, the high volatility and the low electrical conductivity of the arsenic did not hinder the electrochemical or thermal steps.

Successive layers in a InGaSb sample¹⁰⁷ were deposited in the following order: Sb, In, and Ga. Antimony was deposited from a solution of SbCl_3 , H_2SO_4 , and HCl, and then, indium was deposited from a bath containing InCl_3 and KCl at -0.85 V vs. SCE, at room temperature under stirring. Finally, gallium was deposited at -2.00 V vs. SCE from a solution of GaCl_3 and KOH at 47°C . In the deposited InGaSb, the amount of Ga + In (in moles) was equal to that of Sb.

CuInSe_2 thin film was formed by the sequential electrodeposition of Cu and In-Se.¹¹⁴ A Cu layer on a Mo substrate was electrodeposited from a copper sulfate solution,¹¹⁵ followed by an In-Se layer from a solution of indium sulfate and selenious acid.¹¹⁰

CuInSe_2 alloy films on ITO substrates were formed by sequential deposition and thermal treatment.¹¹⁶ The deposition of CuIn films was carried out from an aqueous solution of CuSO_4 and $\text{In}_2(\text{SO}_4)_3$ at a constant applied potential of -0.75 V vs. Ag/AgCl. For the deposition of the Se layer on the previously prepared CuIn alloy film, a constant potential of -0.6 V was applied and an aqueous solution of H_2SeO_3 was used.

Friedfeld *et al.*¹¹⁷ prepared $\text{CuIn}_x\text{Ga}_{1-x}\text{Se}_2$ (CIGS) polycrystalline thin films using a two-step electrodeposition process that involved the electrodeposition of a CuGa precursor film on a molybdenum substrate, followed by the electrodeposition of a CuInSe thin film. The deposition of CuGa films was carried out from a solution containing CuSO_4 , $\text{Ga}_2(\text{SO}_4)_3$, and NaOH at -1.95 V vs. SCE for 2 min using a 500 rpm rotating disk electrode. This CuGa precursor film was coated with a CuInSe overlayer film in a bath containing CuSO_4 , $\text{In}_2(\text{SO}_4)_3$, SeO_2 , and sodium citrate at a potential of -1.2 V vs. SCE for 5 or 10 min. The resulting films showed good crystallinity.

The fabrication of CIGS layers using a two-step electrodeposition process was reported by R.N. Bhattacharya.¹⁰¹ This study indicated that Cu-rich CIGS thin film was electrodeposited first, followed by the electrodeposition of In-Se thin film. The first layer of Cu-rich CIGS thin film was electrodeposited onto an Mo-coated glass substrate from CuCl_2 , InCl_3 , GaCl_3 ,

H₂SeO₃, and LiCl dissolved in a pH 3 buffer solution at a constant potential of -1.0 V (vs. Pt pseudoreference). The subsequent second layer of the InSe thin film was electrodeposited from a solution mixture of In₂(SO₄)₃, sulfamic acid, and LiCl. After annealing in a Se atmosphere, the film composition was Cu_{0.97}In_{0.70}Ga_{0.33}Se₂. Bhattacharya concluded that the deposited Cu layer facilitated the electrodeposition of the subsequent In, Ga, and Se layers.

2.2. Galvanostatic deposition

2.2.1. One-step deposition

2.2.1.1. Binary alloys

Walsh and Gabe⁸⁾ investigated the galvanostatic deposition of indium alloys. InPb alloy was codeposited in a solution containing a suitable complexant. The current densities were in a range between 1 and 3 A dm⁻², and the indium contents of the alloys were 1-60%. The codepositions of InSn alloys from a sulfate solution with cetyltrimethylammonium bromide (CTAB), an acidic fluoborate solution, and perchlorate-cellosolve solutions were carried out at current densities of 1-5 A dm⁻². AgIn alloys were codeposited at current densities of 0.3, 0.5, and 1.5 A dm⁻². InNi alloys with In contents of 13-87% were electrodeposited at a current density of 2 A dm⁻². When the InZn alloy was deposited in an ammonium tartrate solution at current densities of 0.5-1.0 A dm⁻², the alloy behaved as if it were a heterogeneous mixture. InSb alloys were produced from tartrate solutions or from solutions to which polyethylene-polyamine (PEPA) was added at current densities that ranged from 0.5 to 6.0 A dm⁻². For the deposition of alloys containing indium, complexing was essential in order to equalize the deposition potentials.

Vinogradov *et al.*⁴²⁾ studied the electrochemical deposition of InPd. The polarization curves of InPd alloy showed a current maximum at a potential between -0.6 and -0.7 V vs. SHE. InPd alloy depositions were carried out using electrolytes of Pd²⁺, In³⁺, ammonium sulfate, monosodium citrate, ammonium chloride and saccharin in current densities of 50 to 150 A m⁻² at a pH of 8.5 to 9.5, and at 20°C. Alloys with constant indium contents of 20% were deposited.

Dobrovolska *et al.*^{120,121)} performed the electrodeposition of AgIn alloys under galvanostatic conditions. For the galvanostatic electrodeposition of AgIn, the current densities were between 0.2 and 1.1 A dm⁻². The increase in current density led to an increase in

indium content in the alloy, which led to the formation of Ag₃In, Ag₉In₄, and AgIn₂ phases that were richer in indium.

Peristaya *et al.* studied the galvanostatic electrodeposition of InCd alloy. InCd alloys were deposited from a chloride-sulfate solution with tartrate, polyacrylamide, and ammonia,¹²²⁾ and from a sulfate acidic solution containing surfactants.¹²³⁾ In a chloride-sulfate solution, the alloy should be deposited at a pH of 2.5-3.0, at room temperature, and at a current density of 0.75-1.0 A dm⁻². In a sulfate solution with surfactants, the deposition was carried out at room temperature and at a cathodic current density of 1 to 1.25 A dm⁻². They showed that the ratio of the metal content in the InCd alloy depended on the ratio of the metal ion content in the solution, the current density, the temperature, the pH, and the surfactant used. The dependence of the metal content ratio in the alloy on that in the bath (with surfactants) fitted the Akhumov-Rosen equation:

$$\log\left(\frac{[\text{In}]}{[\text{Cd}]}\right) = -0.23 + 1.16 \log\left(\frac{[\text{In}^{3+}]}{[\text{Cd}^{2+}]}\right) \quad (7)$$

Indium-thallium alloys were deposited galvanostatically from an aqueous sulfate solution by Sadana,¹²⁴⁾ who studied the effects of current density and temperature on the composition and appearance of the alloy deposits. InTl alloys containing up to 84.1% indium were electrodeposited from five different solutions in which the total metal content (In + Tl) was kept constant. The current density was varied from 1.0 to 32.0 A dm⁻². An increase in current density decreased the percentage of Tl in the deposit. At a current density of 8.0 A dm⁻², an increase in temperature decreased the percentage of indium in the deposit, but at a current density greater than the limiting current density, the effect of temperature on the composition of the alloy deposit was not significant.

Perelygin *et al.*¹²⁵⁾ reported the electrodeposition of InPb alloys from an acetic electrolyte containing a surfactant. The alloys were deposited at a current density of 0.5 A dm⁻², a temperature of 20-30°C, and a pH of 4-5. They recommended an electrolyte that contains lead acetate (5-10 g/L in terms of lead), indium nitrate (5-10 g/L in terms of indium), sodium acetate (100 g/L), acetic acid (100 mL/L), and a surfactant (0.2 g/L), in order to obtain smooth, dense fine-crystalline deposits of In-Pb alloys with indium contents of up to 80%.

InP films on titanium cathodes were prepared via electrodeposition from an aqueous solution containing InCl_3 and NH_4PF_6 .¹²⁶⁾ InP consisting of 49% indium and 51% phosphorus was prepared for a specific solution composition of 1.25 mM InCl_3 and 58.6 mM NH_4PF_6 using a constant current density of 20 mA cm^{-2} at 22°C with stirring.

Sadana and Singh investigated InSb alloy codeposition from aqueous solutions containing citrate complexes of antimony and indium.¹²⁷⁾ The plating baths for codeposition were prepared by mixing Sb^{3+} , In^{3+} , citric acid, and potassium citrate. The effect of the current density on the deposit composition was studied. With an increase in current density, the percentage of antimony in the deposit first decreased, and then remained constant ($> 6.0 \text{ A dm}^{-2}$). The initial decrease in the percentage of antimony in the deposit became more pronounced with an increase in the indium concentration of the electrolyte.

Sadana and Wang¹²⁸⁾ showed that InBi alloys could be obtained from aqueous solutions with a pH of 1.2, containing 5.0 g/L of Bi, 25.0 g/L of In, and 42.0 g/L of diethylenetriaminepentaacetic acid (DTPA) at current densities of 2.0-8.0 A dm^{-2} . At current densities higher than 8.0 A dm^{-2} , the composition of the deposit remained constant. As the current density increased, the percentage of indium in the deposit increased. X-ray analysis of the original and annealed deposits showed the existence of two intermediate phases. The first was InBi, while the second was assumed to be In_3Bi as a new intermediate phase.¹²⁸⁾

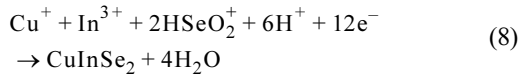
Igasaki and Fujiwara⁵⁰⁾ prepared InSe films via galvanostatic deposition. The plating bath for the deposition of InSe alloy consisted of an aqueous solution containing InCl_3 and SeO_2 . Electrodepositions of InSe alloys were carried out in a constant current range from 3 to 30 mA cm^{-2} at 25°C and a pH of 1. For the deposition of homogeneous InSe films, this study found that a current density of 20 mA cm^{-2} was most suitable. Aksu *et al.*¹²⁹⁾ studied the electrochemical codeposition of InSe thin films from solutions containing indium chloride, selenious acid, and tartrate as a complexing agent. The In/Se ratio in the deposit layer was 2/3 when deposition was performed in a solution of 0.05 M In^{3+} and 0.1 M Se^{4+} at a current density of 10 mA cm^{-2} and a pH of 11.5. The selenium ratios in the alloy films increased with a higher selenium concentration in the solution, a lower pH, and lower current densities.

Herrero and Ortega¹¹⁵⁾ prepared CuIn alloys for the formation of CuInS_2 . In the plating bath for codeposition, CuSO_4 , $\text{In}_2(\text{SO}_4)_3$, and citric acid were mixed. The results of the codepositions showed that stoichiometric deposits (CuIn) were obtained with a 0.7 Cu/In ratio in solution at a current density of 7 mA cm^{-2} . The composition of the electrodeposited Cu-In thin films was a function of the $[\text{Cu}]/[\text{In}]$ ratio in the bath solution and was a function of the applied current density. Ishizaki *et al.*¹³⁰⁾ reported the codeposition of copper and indium. The plating conditions for their example were the following: a bath composition of 0.05 M CuSO_4 , 0.1 M $\text{In}_2(\text{SO}_4)_3$, and 1 M citric acid, a pH of 3.0, a current density of 150 A m^{-2} , and 298 K. They observed the XRD pattern of a 50Cu-50In alloy deposit. Zarubitskii *et al.*³⁶⁾ studied the joint deposition of copper and indium obtained by galvanostatic deposition. The optimal contents of the components of the plating solution for the deposition of a lustrous gold-colored CuIn alloy coating were as follows (g/L): 8-12 $\text{CuSO}_4 \cdot 5\text{H}_2\text{O}$, 2.5-5.0 $\text{In}_2(\text{SO}_4)_3$, 100-160 potassium sodium tartrate ($\text{NaK}[\text{C}_4\text{H}_4\text{O}_6] \cdot 4\text{H}_2\text{O}$), 25-30 Trilon B, 30-35 NaOH, 15-30 Na_2SO_4 , 15-25 glycerol, and 0.05-0.2 gelatin. The electrolysis mode was a cathodic current density of 0.4-0.6 A dm^{-2} , an anodic current density of 0.15-0.40 A dm^{-2} , a temperature of 20-25°C, and a pH of 13.4-13.6. The bath solutions were stirred during electroplating. The deposited alloys contained 79-81% copper and 19-21% indium. According to this study, the main parameters determining the color and quality of the deposit were the cathodic current density and the concentration of $\text{In}_2(\text{SO}_4)_3$.

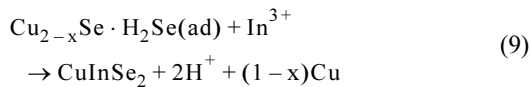
2.2.1.2. Ternary and quaternary alloys

Sahu *et al.*¹³¹⁾ reported the cathodic electrodeposition of CuInSe_2 thin films on Mo cathodes from aqueous solutions containing CuCl , InCl_3 , and SeO_2 . Reproducible and stoichiometric CuInSe_2 films were obtained at a constant current density of 6 mA cm^{-2} (-0.4 V vs. SCE) for 15 min at a temperature of 23°C and a pH of 1.0. Annealing experiments were carried out both in a vacuum and air at various temperatures. In the deposition of CuInSe_2 , it was considered that initially, Se and Cu might react to give CuSe or CuSe_2 . Then, with the simultaneous deposition of Cu, In, and Se, the formation of CuInSe_2 was likely. They reported that the presence of an HSeO_2^+ ion was identified (pH 1) through cyclic voltammetry measurement from an aqueous solution of Cu^+ , In^{3+} , Se^{4+} , and they suggested

the following mechanism, including the HSeO_2^+ ion:



It is important that indium is deposited by an underpotential reaction, and that its deposition is always preceded by the deposition of Cu_2Se (or Cu_{2-x}Se) in CIS electrodeposition.^{71,91,132,148} Mishra and Rajeshwar¹³² proposed that the first stage of the mechanism of CIS codeposition was the formation of Cu_{2-x}Se . This mechanism, however, included not HSeO_2^+ but H_2Se . They employed an electrodeposition bath similar to the one employed by Ueno *et al.* (in a solution of Cu^{2+} , In^{3+} , and SO_4^{2-} with pH 1, at -0.8 V vs. SCE and at $50\text{--}55^\circ\text{C}$).⁶⁴ The mechanism involved the concurrent formation of Cu_{2-x}Se , then its subsequent reduction, coupled with the reduction of H_2SeO_3 to H_2Se , and finally the underpotential assimilation of In^{3+} into the solid phase, leading to CuInSe_2 . The following reaction is a general representation of the mechanism for the deposition of CuInSe_2 .



Thin films of copper indium sulfoselenide ($\text{CuInS}_x\text{Se}_{2-x}$) were prepared using the galvanostatic deposition technique by Garg *et al.*¹³³ The electrolyte bath mixture consisted of 10 mL CuCl (2.5 mM), 10 mL InCl_3 (16 mM), 10 mL citric acid (0.25 M), 10 mL sodium selenosulfate ($\text{Na}_2\text{O}_3\text{SSe}$, 2 mM), 10 mL ($\text{Na}_2\text{S}_2\text{O}_3$), and 10 mL NH_4OH . The pH level of the bath solution was greater than 9. Electrodeposition onto ITO glass substrates was carried out for 15 min in a galvanostatic mode in an unstirred solution at room temperature. They obtained indium-rich $\text{CuInS}_x\text{Se}_{2-x}$ films at a current density of ~ 1.0 mA cm^{-2} .

2.2.2. Multi-step deposition

2.2.2.1. Binary alloys

Chu *et al.*¹³⁴ prepared CuIn films using a sequential electrodeposition technique for CuInSe_2 formation. They performed the electrodeposition of copper before the deposition of indium, due to the reaction of indium with copper in the plating solution. The electroplating of Cu was carried out from a sulfuric acid solution of copper sulfate at a current density of $50\text{--}75$ mA cm^{-2} . The electrodeposition of In was carried out from a sul-

furic acid solution of indium sulfamate and sodium sulfamate (pH = 1.5 – 2) at a current density of $10\text{--}20$ mA cm^{-2} . Huang *et al.*¹³⁵ reported the electrodeposition of indium on copper in an acidic sulfate solution. In their study, a copper layer was plated on the PVD Cu seed prior to the indium electrodeposition. One of two Cu plating solutions was used to electroplate the Cu underlayer: (1) a citrate copper solution with a pH of 5.6 containing 75 mM CuSO_4 and 0.25 M sodium citrate, and (2) a typical commercial damascene copper chemistry that contained 0.6 M CuSO_4 , 0.1 M H_2SO_4 , 1.4 mM HCl, along with a suppressor (polyethylene glycol, PEG) and an accelerator (bis(sodium-sulfopropyl) disulfide, SPS).¹³⁶ The Cu layers were electroplated from the citrate chemistry at a current density of -5 mA cm^{-2} . Indium electrodeposition was carried out at 20°C , in solutions containing 44 mM $\text{In}_2(\text{SO}_4)_3$ and 0.5 M Na_2SO_4 at a current density of -0.5 mA cm^{-2} or -5 mA cm^{-2} . A natural solution with a pH of about 2.4 was used. According to their conclusions, the room temperature alloy formation promoted the conformal deposition of a few monolayers of alloy, and the rapid interdiffusion between Cu and In further extended this alloy formation to a thicker layer, and delayed the typical island formation-growth phenomenon.

InSb intermetallic compounds were formed by the galvanostatic electrodeposition of indium onto antimony-deposited Fe substrates as cathodes.¹³⁷ The antimony-deposited Fe substrate, either crystalline or amorphous, was prepared by galvanostatic electrodeposition from an aqueous solution containing 0.3 M SbCl_3 , 1.6 M H_2SO_4 and 1.7 M HCl. Crystalline Sb deposits were obtained from electroplating baths with or without the surface-active agent, Trilon B of 40 g/L. The bath for indium deposition was an aqueous solution of 0.67 M, InCl_3 and a pH of 1.3 or 1.7. Electrodepositions of In were carried out at room temperature and at current densities ranging from 1.77 to 20 A dm^{-2} . The influence of the type of antimony substrate on the diffusion and reaction process of an electrodeposited indium overlayer was investigated.

2.2.2.2. Ternary and quaternary alloys

CuIn and CuInGa thin films were prepared via the galvanostatic deposition of metallic components.¹³⁸ First, a layer of copper was deposited onto an Mo-sputtered glass plate from an acidic aqueous solution of CuSO_4 at room temperature. A layer of indium was

then electrodeposited on top of the already-plated copper film from an aqueous solution of indium sulfamate ($\text{In}(\text{SO}_3\text{NH}_2)_3$). The $[\text{Cu}]/[\text{In}]$ ratio was maintained in the range of 0.95 to 0.98 in order to obtain single-phase CuInSe_2 . To introduce gallium, gallium was electroplated on top of the already-plated film of indium so that the $[\text{Cu}]/([\text{In}] + [\text{Ga}])$ ratio was maintained at 0.95-0.98.

Electrodeposited CuInGaSe_2 layers were prepared by a three-stage electrodeposition process.¹³⁹ Electrodeposition of CIGS on an Mo-coated glass substrate was performed from a bath containing 0.05 M CuCl_2 , 0.06 M InCl_3 , 0.03 M H_2SeO_3 , 0.1 M GaCl_3 , and LiCl (pH 2-3) by applying a constant current density of 0.9 mA cm^{-2} for 10 min. The subsequent second Cu layer was electrodeposited from a 0.1 M CuSO_4 solution at a constant current density of 8.2 mA cm^{-2} for 3 min. The third In layer was electrodeposited from a 0.1 M InCl_3 solution at a constant current density of 7.2 mA cm^{-2} for 6 min. All films were deposited at room temperature without stirring. The researchers were able to fabricate 10.9%- efficient CIGS-based solar cells by electrodeposition.

2.3. Deposition onto a metal substrate that is one component of an alloy

Kozlov *et al.* reported that InSb intermetallic compounds were formed by the galvanostatic deposition of indium onto an antimony metal substrate.¹⁴⁰ The bath condition for the indium deposition and the galvanostatic deposition condition were the same as that described in ref. 137.

Canegallo *et al.*¹⁴¹⁻¹⁴³ studied indium electrodeposition on bismuth cathodes at a constant current density and at a temperature of 25-70°C, which gave rise to the formation of three intermetallic compounds. The bath solution was an aqueous solution of 0.67 N InCl_3 and pH 1.3. Two wires made of indium were used as the anode and the reference electrode. Experiments were carried out at current densities ranging from 2.4 to 21.6 A m^{-2} and with deposition times ranging from 1.2 to 8.3 h.

2.4. Potential or current pulse deposition

Sonu and O'Keefe¹⁴⁵ prepared indium-thallium alloys, which are known as shape memory alloys. InTi alloys in the range of 15-38 at% Tl were electrodeposited from a sulfate electrolyte using a pulsed current. To obtain alloys of different composition, changes

were made in various pulse parameters, such as the peak current density, pulse frequency, and duty cycle. Uniform, dense alloy deposits with the desired thallium content could be produced by using a peak current density of $10\text{-}40 \text{ mA cm}^{-2}$, with 10 ms as the on time, and a duty cycle of about 30% at room temperature. In pulse electrodeposition, the pulse period, T , is the sum of the on-time and off-time ($T = t_{\text{on}} + t_{\text{off}}$), and the duty cycle, θ , is the ratio of the on-time to the pulse period ($\theta = t_{\text{on}}/(t_{\text{on}} + t_{\text{off}}) \times 100\%$). Deformed InTi alloys with a 21-28 at% Tl composition at 25°C recovered their original shape upon heating.

Yang *et al.*¹² fabricated InSb nanowire arrays by pulsed electrodeposition. The deposition was performed into an Au-sputtered anodic alumina membrane (AAM) from an electrolyte solution with a pH of 2.2 that contained InCl_3 , SbCl_3 , and citric acid at 20°C, at a potential of $V_{\text{on}} = -2.1 \text{ V}$. It was found that the InSb alloys had a zinc-blende structure and were single-crystalline.

Electrodeposition of CIGS films on an Mo/glass substrate was performed at room temperature without stirring.¹⁴⁶ The electrolyte bath contained 3 mM CuCl_2 , 10 mM InCl_3 , 10 mM GaCl_3 , 8 mM H_2SeO_3 , and 60 mM sodium sulfamate as a complexing agent. The pH of the solution was 2.10-2.20. The deposition of the CIGS films was carried out with a square-pulse potential, where the nonpulse potential was constant at 0.0 V vs. SCE and the pulse potential was constant at -0.6 V . The pulse period, T , was 3 s, and the duty cycle, θ , varied from 33 to 100%. The deposition time was 60 min.

Vertically aligned arrays of CuInSe_2 nanowires of controllable diameter and length were synthesized by pulse cathodic electrodeposition from an acidic solution into anodized alumina (AAO) templates, followed by annealing at 220°C in a vacuum.¹⁴⁷ The bath solution was a mixture of 1.5 mM CuSO_4 , 2 mM $\text{In}_2(\text{SO}_4)_3$, 3.5 mM H_2SeO_3 , and LiCl , in an aqueous buffer solution (pH 2.8) containing potassium hydrogen phthalate and HCl . The optimized pulse waveform with a pulse time of $t_{\text{on}} = 0.3 \text{ s}$ at a potential $V_{\text{on}} = -1 \text{ V}$ (w.r.t. platinum counter electrode) and a discharge time of $t_{\text{off}} = 2 \text{ s}$ at $V_{\text{off}} = 0 \text{ V}$ yielded dense and compact CIS nanowires.

2.5. Sequential electrodeposition under potentiostatic and galvanostatic conditions

CuIn alloys were deposited by sequential electrodeposition.¹¹⁵ First, copper was deposited onto a Ti

substrate from citrate electrolytes containing 0.01 M of CuSO_4 and 0.25 M of a citric acid-citrate buffer with a pH of 4, at -0.5 V vs. SCE, using a copper anode in order to maintain the Cu^{2+} concentration in the electrolyte. Indium was then plated onto the copper layer from a solution that contained 0.1 M $\text{In}_2(\text{SO}_4)_3$ and 0.4 M citric acid with a pH of 2 under galvanostatic conditions of 5 mA cm^{-2} . In this deposition, the formation of intermetallic Cu_7In_4 was observed.

2.6. Heat treatment with gaseous nonmetallic compounds or elementary nonmetal vapors

In-P, In-S, and In-Se layers were obtained by annealing indium-deposited substrates in gaseous element flows. The electrodepositions onto Ti substrates of In were performed from $\text{In}_2(\text{SO}_4)_3$ solutions at a constant potential of -1.4 V vs. SCE¹¹⁸⁾ and -1.0 V vs. SCE.¹¹⁹⁾ Thin InP layers were prepared by the electrodeposition of In films onto Ti substrates followed by annealing in a PH_3 flow.^{41,119)} In_2S_3 films were obtained by the heat treatment of the electrodeposited In films in a flowing stream of H_2S at 350°C .¹¹⁸⁾

$\text{InAs}_x\text{P}_{1-x}$ layers were prepared by the codeposition of InAs alloys and annealing under PH_3 at 500°C and subsequently at 600°C .⁴⁵⁾

For the preparation of CIS or CIGS, CuIn or CuInGa films have sometimes been chalcogenized by heat treatment in a flow of $\text{H}_2\text{S}(\text{Se})$,^{56,104,115)} $\text{H}_2\text{S}(\text{Se}) + \text{Ar}$,^{56,138)} or under an elementary S(Se) atmosphere.^{59,97,104)} Annealed CIS or CIGS films have also been etched in KCN solution in order to remove CuS phases.⁵⁹⁾

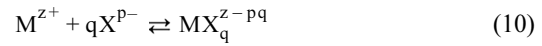
2.7. Electrochemical and photochemical deposition

Rabchynski *et al.*¹⁴⁴⁾ prepared In_2Se_3 nanoparticles via the illumination of an Se electrode in an acidic aqueous In^{3+} solution. Selenium film was galvanostatically deposited onto Au in an aqueous solution containing 5 M SeO_2 and 9 M H_2SO_4 at a current density of 1 mA cm^{-2} at $95 \pm 2^\circ\text{C}$. In_2Se_3 particles were prepared via the illumination of an Se electrode in a solution of $\text{In}(\text{NO}_3)_3$ in 0.1 M HNO_3 at a potential of -0.2 V vs. Ag/AgCl, at $18 \pm 2^\circ\text{C}$. To prevent bulk indium deposition, the applied potential was more positive than the equilibrium potential $E_{\text{In(III)/In(0)}}$. In an acidic In^{3+} solution with a concentration lower than 0.01 M, the illumination of an Se electrode for 5-7 min at the cathodic potential (-0.2 V vs. Ag/AgCl) resulted in the formation of an orange turbid colloidal solution.

The In_2Se_3 particles were not uniformly distributed in size, and the majority of the particles had sizes from 40 to 80 nm and shapes that were mainly spherical. The colloid of In_2Se_3 was stable for 12-18 h, and thereafter, sedimentation was observed.

3. Additives

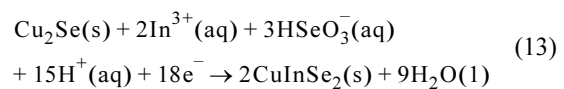
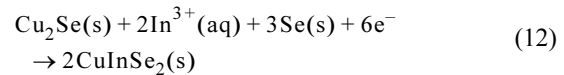
A complexing agent (complexant) that forms a complex ion with one of the discharging metal ions is known to change the deposition potential. Let us assume a complexing ion X^{p-} that is present in the bath is complexed with an ionic species, M^{z+} , as follows:

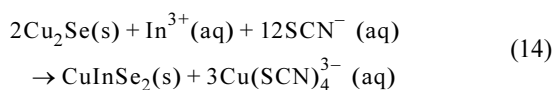


Its reduction equilibrium potential is then shifted according to the Nernst equation

$$E = E_{\text{M}^{z+}}^0 - \frac{RT}{zF} \ln k^* + \frac{RT}{zF} \ln \left[\frac{(a_{\text{MX}_q^{z-pq}})}{(a_{\text{X}^{p-}})^q} \right] \quad (11)$$

where k^* is the stability constant of the complex, and MX_q^{z-pq} and $a_{\text{X}^{p-}}$ are the activities of MX_q^{z-pq} and X^{p-} , respectively. A complexant helps in bringing the deposition potentials of two or more species near to one another for codeposition. An example of codeposition using a complexant is that of CuInSe_2 , for which thiocyanate ion (SCN^-) was used.¹⁴⁸⁻¹⁵⁰⁾ Kemell *et al.* showed that the use of SCN^- as a complexing agent shifted the reduction potential of the Cu^+ ion to a more negative value; however, the effects of SCN^- on the reduction potentials of In^{3+} and Se^{4+} were not significant. They confirmed that the formation of CuInSe_2 proceeded via the codeposition mechanism that was induced at more positive potentials than those at which Cu^+ or In^{3+} alone was reduced. The reaction seemed to proceed via Cu_{2-x}Se formation because no In_ySe compounds could be deposited in the potential range in which CuInSe_2 formation was observed. They suggested that the formation of CuInSe_2 might proceed according to one of the following reactions:





The mechanisms involving H_2Se (Eq. 9)¹³²⁾ seemed to be impossible under the SCN^{-} bath condition because the stoichiometric potential region for CuInSe_2 formation extended to such positive potentials at which H_2Se formation was quite unlikely.

The potentiostatic deposition of a ternary CuInSe system was investigated by Ganchev *et al.*⁶¹⁾ Electrodeposition onto an ITO glass was carried out from an aqueous solution containing 2.75 mM CuCl , 1.3 mM $\text{In}_2(\text{SO}_4)_3$, 3 mM SeO_2 , and 4 M KSCN in a potential range of -0.7 V to -1 V vs. SCE. The results showed that thiocyanate ions could be used as a suitable complexing agent. The stability constants for the complex formation of Cu^{+} and In^{3+} ions with SCN^{-} ions are listed in Table 5.

Ishizaki *et al.* examined the effect of complex forming reagents, citric acid, and EDTA for the codeposition of CuIn .¹³⁰⁾ The experimental results were as follows:

When citric acid or EDTA was added, the deposition potentials for Cu and In shifted toward more negative potentials and their limiting current densities were reduced.

Stoichiometric CuIn alloys were deposited from solutions containing citric acid at lower current densities as compared to the solutions of EDTA.

The electrodeposition of Ag-In alloy from a cyanide electrolyte with D(+)-glucose was studied.¹²¹⁾ The cathodic depositions of Ag, In, and Ag-In alloy onto platinum sheets in the cyanide electrolyte occurred at potentials of -970 mV, -1970 mV, and -1170 mV vs. Ag/AgCl, respectively.

Whang *et al.* studied the influence of complexing

agents on the reduction potentials for the one-step electrodeposition of CuInSe_2 .^{151,152)} They analyzed cyclic voltammograms of individual metal ions and mixtures of Cu^{2+} , In^{3+} , and Se^{4+} , using triethanolamine and citrate as complexing agents, and without any complexing agent. They concluded that the application of citrate as a complexing agent in the electrodeposition of CuInSe_2 provided a feasible environment. Citrate shifted the deposition potential of the copper ion in a negative direction that was closer to that of the indium ion and promoted the formation of crystalline films of CuInSe_2 .

Solorza-Feria *et al.* investigated the effect of citrate ion concentration on the photoresponse of p- CuInSe_2 that was electrodeposited from citrate complexes.⁸⁰⁾ The best photocurrent was obtained from thin films that were electrodeposited using 0.06 M sodium citrate.

Table 6. Complexing agents used for In alloy deposition

Alloys	Complexing agents
AgIn	Cyanide ^{120,121,154)}
InBi	Diethylenetriaminepentaacetate (DTPA) ¹²⁸⁾
InCd	Tartrate ¹²²⁾
InZn	Tartrate ⁸⁾
InPb	Acetate ¹²⁵⁾
InPd	Ammonium-Citrate ⁴²⁾
	Triethanolamine, ⁵⁶⁾
CuIn	Ethylenediaminetetraacetate (EDTA), ¹³⁰⁾
	Trilon B-Tartrate, ³⁶⁾ Citrate ^{57,97,115,130,135)}
InSn	Cetyl trimethyl ammonium bromide (CTAB) ⁸⁾
InSb	Tartrate, ⁸⁾ Citrate, ^{12,41,46-48,127)} Trilon B ¹³⁷⁾
InAs	Citrate, ^{41,45)} Ethanolamine ⁹⁶⁾
In_2Se_3	Tartrate, ¹²⁹⁾ Citrate-Ethanolamine ¹¹⁰⁾
$\text{InAs}_{1-x}\text{Sb}_x$	Ethanolamine ⁹⁶⁾
	Triethanolamine, ^{29,60)} EDTA, ⁸⁵⁾
CuInSe_2	Diethylenetriamine, ⁸⁹⁾ Thiocyanate ^{61,62,148-150)} , Citrate ^{65-67,69,73,80-83,87,88,90,113)}
CuInS_2	Triethanolamine ^{40,56)}
CuInGa	Citrate ⁹⁷⁾
CuInTe_2	Triethanolamine ⁶⁰⁾
$\text{CuIn}_x\text{Ga}_{1-x}\text{Se}_2$	Citrate, ^{88,90)} Sulfamate ^{101,104,146)}
$\text{CuInS}_x\text{Se}_{2-x}$	Citrate ¹³³⁾
CuInSeTe	Citrate ¹⁰⁶⁾
$\text{Cu(In,Ga)}(\text{S}_2\text{Se})_2$	Sulfamate ¹⁰⁴⁾

Table 5. Stability constants for Cu^{+} and In^{3+} complexes⁶¹⁾

Reaction	log k*
$\text{Cu}^{+} + \text{SCN}^{-} \rightleftharpoons \text{CuSCN}$	12.7
$\text{Cu}^{+} + 2\text{SCN}^{-} \rightleftharpoons \text{Cu}(\text{SCN})_2^{-}$	11.0
$\text{Cu}^{+} + 3\text{SCN}^{-} \rightleftharpoons \text{Cu}(\text{SCN})_3^{2-}$	11.6
$\text{Cu}^{+} + 4\text{SCN}^{-} \rightleftharpoons \text{Cu}(\text{SCN})_4^{3-}$	12.02
$\text{In}^{3+} + \text{SCN}^{-} \rightleftharpoons \text{In}(\text{SCN})^{2+}$	2.6
$\text{In}^{3+} + 2\text{SCN}^{-} \rightleftharpoons \text{In}(\text{SCN})_2^{+}$	3.6
$\text{In}^{3+} + 3\text{SCN}^{-} \rightleftharpoons \text{In}(\text{SCN})_3$	4.6

Walsh and Gabe⁸⁾ showed that various complexing agents have been used for the galvanostatic deposition of indium alloys. For the electrodeposition of indium alloys including CI(G)S films, among the possible complexing agents, carboxylates such as citrate and tartrate anions, show some advantages over other agents. They form complexes with both indium and copper, which are not toxic or hazardous, and they can be used to buffer the pH solution.⁶⁶⁾ These agents for the electrodepositions of indium alloys are listed in Table 6.

In Table 6, the term “citrate” as a complexing agent indicates “citric acid and/or citrate.”

4. Substrates

For the electrodeposition of alloys and semiconductors containing indium, a variety of cathodic substrates can be used, depending on the purpose of the thin films. For metallic alloys, metallic plates are mainly used, and conducting glass substrates are used for the absorber layers of photovoltaic cells such as CIS and CIGS. Electrode materials sometimes have an influence on the properties of alloy thin films.

Bhattacharya and Rajeshwar⁶⁰⁾ prepared CuInSe₂ thin films on ITO and Mo substrates, which yielded different composite films. The atomic ratios of Cu/In/Se were 31.31:20.02:48.67 for an ITO substrate, and 22.38:22.98:54.64 for a Mo substrate. The researchers attributed the difference in the compositions for ITO and Mo to the different overpotentials on the substrates' surfaces.

The influence of the substrate on the orientation and surface morphology of CuInSe₂ was reported by Gujar *et al.*¹⁵³⁾ For the deposition of CuInSe₂ thin films, aqueous solutions of CuSO₄, In₂(SO₄)₃, and H₂SeO₃ were combined together in a 1:1:1 ratio. The solution pH was maintained at 1.5-2.0. The electrodeposition of CuInSe₂ thin films was carried out on tin-doped indium oxide (ITO), fluorine-doped tin oxide (FTO), Ni, Mo, and stainless steel (SS) substrates at constant potentials ranging from -600 to -1000 mV vs. Ag/AgCl for 20 min without stirring. No significant change in orientation or in the crystalline nature of the CuInSe₂ films was observed for different substrates, but a slight change in the crystallite size and surface morphology of the CuInSe₂ films as a function of the substrate was observed. The CuInSe₂ film on the ITO substrate exhibited clustering of nuclei that were of a

uniform size and were cauliflower-shaped. The CuInSe₂ film on the FTO substrate showed larger particles that were cauliflower-shaped. The grain size on the Ni and SS substrates was smaller than those on the ITO and FTO substrates. The films on Ni and SS were very compact, and nanograin-like morphologies were observed on the Ni and SS.

The differences between the electrodepositions on

Table 7. Cathodic electrode substrates in the electrodeposition of In alloys

Alloys	Substrates
AgIn	Cu, ¹²⁰⁾ Pt ^{121,154)}
InBi	Stainless steel (SS), ¹²⁸⁾ Bi ¹⁴¹⁻¹⁴³⁾
InPb	Cu ¹²⁵⁾
InTl	Glassy carbon ¹⁴⁵⁾
InZn	Al, ⁴³⁾ Vitreous carbon ⁴⁴⁾
CuIn	Cu, ³⁶⁾ Ni, ⁵⁷⁾ Ti, ^{56,57,59,115,130)} Mo-coated glass, ^{58,97,138)} W-coated graphite, ¹³⁴⁾ Si/TaN/Ta/Cu ¹³⁵⁾
InP	Ti ¹²⁶⁾
InSb	Ti, ^{41,46)} Cu, ⁴⁶⁾ Cu-coated Si, ⁴⁷⁾ Si, ⁴⁷⁾ ITO, ⁴⁶⁾ Ni-coated Cu, ⁹⁶⁾ Fe, ¹³⁷⁾ Sb, ¹⁴⁰⁾ Au-coated AAM (anodic alumina membrane) ^{12,48)}
InAs	Ti, ^{41,45)} Ni-coated Cu ⁹⁶⁾
In ₂ S ₃	S-modified Au ¹⁰⁹⁾
In ₂ Se ₃	Cu, ⁶⁸⁾ Mo, ⁵²⁾ Ti, ^{49,68,110)} Cu-coated Mo, ⁵²⁾ Ti-coated glass, ⁵⁰⁾ Mo-coated glass, ⁵¹⁾ ITO, ^{49,53-55)} SnO ₂ -coated glass, ⁵¹⁾ SS/Mo/In, ¹²⁹⁾ Au ¹⁴⁴⁾
InAs _{1-x} Sb _x	Ni-plated Cu ⁹⁶⁾
CuInSe ₂	Cu, ⁶⁸⁾ Mo, ^{60,66,67,88,113,131,153)} Ti, ^{64,66,85-87)} Al, ⁸⁹⁾ Ni, ^{80,153)} SS, ^{89,153)} FTO (F-doped SnO ₂ -coated glass), ²⁹⁾ ITO, ^{60,61,80,89,113,116,153)} ITO/CdS, ⁶⁰⁾ CdS, ⁸⁴⁾ Ti-coated glass ⁶⁵⁾ , Mo-coated glass, ^{52,62,68,69,72,74-76,78,79,88-91,102,114,148)} SnO ₂ -coated glass, ^{70-73,77,80-83,85)} Mo-coated alumina, ⁶³⁾ AAO (anodized alumina) ¹⁴⁷⁾
CuInS ₂	Ti ^{40,56,92)}
CuInTe ₂	Mo, ⁶⁰⁾ ITO, ⁶⁰⁾ ITO/CdS, ⁶⁰⁾ SnO ₂ -coated glass ⁹⁵⁾
CuInGa	Mo-coated glass ^{97,138)}
CuIn _x Ga _{1-x} Se ₂	Mo, ^{88,117)} Au-coated AAM, ¹⁰⁵⁾ Mo-coated glass ^{79,88,90,97,100-104,139,146)}
CuInS _x Se _{2-x}	ITO ¹³³⁾
CuInSeTe	Mo-coated glass, ¹⁰⁶⁾ ITO ¹⁰⁶⁾
Cu(In,Ga)(S,Se) ₂	Mo-coated glass ¹⁰⁴⁾

the different type of substrates are mainly due to the different overpotentials at their surfaces. The cathodic electrode substrates used for the electrodeposition of In alloy thin films are shown in Table 7.

5. Post treatment

As-grown electrodeposited films require thermal treatment to improve their physical properties. De Silva *et al.*⁸⁶⁾ showed that CuInSe₂ material became more crystalline with an increase in the annealing temperature up to 350°C, and crystalline SeO₂ formed by annealing at 200°C in air disappeared during annealing at 350°C.

For the electrodeposition of In alloys that contain Se, such as InSe, CIS, and CIGS, the as-grown films showed a small excess of elemental selenium. Heat treatment removed the excess Se and improved the crystallinity and the optoelectronic properties of the materials.⁵¹⁾

Herrero and Ortega¹¹⁰⁾ prepared In₂Se₃ thin films via the sequential electrodeposition of selenium and indium. In₂Se₃ thin films obtained from subsequent thermal treatment at 500°C showed a photovoltaic response, and they were identified as having a b-

In₂Se₃ crystallographic phase, by X-ray diffraction. The films that were annealed at 600°C showed no photoactivity.

Deposited CIS or CIGS films are annealed in a vacuum, Ar (N₂), or the gaseous elements in alloys at 400-600°C, and annealed films are sometimes etched in KCN solution to remove the CuSe(S). Pern *et al.*⁶³⁾ fabricated polycrystalline thin films of CuInSe₂ from a solution containing CuSO₄, In(SO₃NH₂)₃ and H₂SeO₃ via simple one-step electrodeposition and annealing at 200-250°C for 0.5 h, followed by another for 0.5-1 h in flowing Ar at 400°C. Guillén and Herrero⁶⁹⁾ heat-treated CuInSe₂-deposited thin films under an Ar atmosphere at 400°C for 15 min. Chemical etching was performed by immersion in an aqueous 0.5 M KCN solution at 40°C for 2 min. It was found that the combination of thermal and chemical treatments facilitated the improvement of the compositional and optical properties of electrodeposited thin films.

Guillemoles *et al.*⁷⁴⁻⁷⁶⁾ investigated the annealing treatments of electrodeposited CuInSe₂ films in a selenium atmosphere. Annealing treatments under Se pressure transformed these precursor films into large-grain CuInSe₂ films that had improved electronic properties. It was shown that these modifications

Table 8. Heat treatment conditions for indium alloy or semiconductor thin film formation

Alloys	Heat treatment	References
In ₂ Se ₃	Ar, at 390°C	51
	Ar with 30-50 ppm O ₂ , at 500°C	110
InAs	N ₂ , at 400°C	96
InAsSb	N ₂ , at 400°C	96
InGaSb	At 200 or 400°C	107
CuInSe ₂	Ar (or N ₂), at 500°C	29, 60, 89
	Ar (or N ₂), at 400°C	63, 67, 69, 70, 85, 87, 89
	Air at 350°C	80, 86
	Vacuum, at 450°C	88, 90
	Vacuum, at 220°C	147
	Se and Ar, at 400°C	84, 114
	Se and/or In at 400-550°C	74-76, 78, 79, 102
CuInS ₂	Vacuum, at 400°C	92
CuIn _x Ga _{1-x} Se ₂	Se, In and Ga at 550°C	102
	Vacuum, at 450°C	88, 90
	Ar, at 400°C	103
	Ar, at 600°C	117
CuInSeTe	Te, at 550°C and vacuum, 400°C	106

depend on the Se pressure that is imposed during the heat treatment. Their results showed that the presence of excess Se probably induced the formation of a dead layer with a high density of surface state.

For the preparation of CuInSe_2 , Calixto *et al.*⁷⁹⁾ performed potentiostatic codeposition and selenization at 550°C. The film's stoichiometry was improved after selenization. The films were formed with a mixed phase composition of CuInSe_2 and $\text{CuIn}_2\text{Se}_{3.5}$ ternary phases. Fernandez *et al.*⁷⁸⁾ annealed deposited CuInSe_2 film at 550°C in a selenium-indium atmosphere, which resulted in a near-stoichiometric CuInSe_2 composition.

Sebastian *et al.*¹⁰²⁾ prepared $\text{CuIn}_{1-x}\text{Ga}_x\text{Se}_2$ and CuInSe_2 thin films via electrodeposition and thermal processing at 550°C in a vacuum, in which the film's stoichiometry was adjusted by adding In, Ga, and Se vapors. The results of surface analyses showed that the CIS as well as the CIGS possessed a very thin In-rich surface ($\text{CuIn}_2\text{Se}_{3.5}$) n-layer and a p-type Cu-rich bulk region (CuInSe_2). Vapor pressure of Se is low, thus Se needs high temperature annealing step. To maintain the stoichiometry of CI(G)S film, thermal treatments at 400-550°C were performed in Se atmosphere.⁷⁴⁻⁷⁶⁾ Various heat treatment conditions for this In alloy or semiconductor thin film formation are summarized in Table 8.

6. Metal Diffusion during Electrodeposition

In the electrodeposition of an alloy compound, the interdiffusion of one metal to the other metal leads to the formation of different kinds of intermetallic compounds. Canegallo *et al.*¹⁴¹⁻¹⁴³⁾ reported that indium electrodeposition on bismuth cathodes at a constant current density gave rise to the formation of three intermetallic compounds. These compounds were formed as a result of indium diffusion and reaction inside the Bi electrode. At medium to low current densities, the surface was coated with an InBi intermetal-

lic compound; at higher current densities, with In_2Bi , and at the highest current densities, with In. In the results of more accurate investigations of these compounds' composition and structure, the formation of the third intermetallic compound, In_3Bi_3 could be seen.

Huang *et al.*¹³⁵⁾ reported the electrodeposition of indium on copper in an acidic sulfate solution. They proposed a hypothesis that involved CuIn alloy formation and CuIn interdiffusion. They used Cu seed substrates which were deposited by physical vapor deposition ((100)Si/10 nm TaN/10 nm Ta/30 nm Cu seed layer). A copper layer was plated onto the PVD Cu seed prior to the electrodeposition of indium. Based on the cyclic voltammograms, they suggested that most of the Cu could be alloyed with indium. Rapid interdiffusion was observed between the electroplated copper and indium, and a CuIn_2 alloy phase formed during the indium deposition at room temperature. While the alloy formation was believed to promote the conformal deposition of a few indium monolayers, the rapid interdiffusion counterbalanced the indium deposition and lowered the indium content at the surface.

Mengoli *et al.*¹⁰⁷⁾ prepared $\text{In}_x\text{Ga}_{1-x}\text{Sb}$ samples via multi-step electrodeposition and annealing at 200°C or 400°C. The results showed that only $\text{In}_x\text{Ga}_{1-x}\text{Sb}$ samples with $x \geq 0.91$ formed a single phase, while two phases (In-rich and Ga-rich) were detected for lower x values. They suggested that a compound formation could occur through the diffusion of III group metals into the Sb and a solid-phase reaction. Kozlov *et al.* prepared InSb intermetallic compounds via the galvanostatic electrodeposition of indium onto an Sb-deposited Fe substrate¹³⁷⁾ and an antimony metal substrate.¹⁴⁰⁾ The electrodepositions of Sb on Fe were carried out from electroplating baths with or without the surface-active agent, Trilon B.¹³⁷⁾ The indium layers on the Sb substrates annealed at 40-135°C had a three-

Table 9. Indium diffusion coefficient as a function of temperature for different Sb substrates

Temperature (°C)	25	40	70	110	135	140
$D \times 10^{19} \text{ m}^2 \text{ s}^{-1}$, metallic Sb ¹⁴⁰⁾	0.1±0.04		0.58±0.08	1.22±0.10	2.59±0.33	
$D \times 10^{19} \text{ m}^2 \text{ s}^{-1}$, crystalline Sb (with Trilon B) ¹³⁷⁾			0.352±0.245	2.91±1.15		17.6±6.5
$D \times 10^{19} \text{ m}^2 \text{ s}^{-1}$, crystalline Sb (without Trilon B) ¹³⁷⁾		0.204±0.150	2.14±1.05	23.1±8.5		69.2±21.0
$D \times 10^{19} \text{ m}^2 \text{ s}^{-1}$, amorphous Sb ¹³⁷⁾		3.44±1.25	17.1±6.5	112±30		492±90

layer structure of In/InSb/Sb from the surface to the bulk. The formation of InSb was due to the diffusion of indium into the bulk of the cathode (Sb) and to the reaction with antimony. They determined the diffusion coefficient of indium in InSb as a function of the time following indium deposition and of the annealing temperature. They also studied the influence of the type of Sb substrate on the diffusion coefficient of indium in the alloy. The values of D at the different temperatures used and on the different Sb substrates are presented in Table 9.

7. Properties of Electrodeposited Thin Films as Related to Electrodeposition Parameters

Many researchers have studied the effects of applied potentials or currents. Bhattacharya *et al.*⁵²⁾ analyzed InSe films using EPMA (electron microprobe analysis). Their results showed that InSe-deposited films obtained at -0.9 V vs. SCE were $\text{In}_{1.80}\text{Se}_3$ and that the InSe films at -1.1 V were $\text{In}_{1.92}\text{Se}_3$. At potentials lower than -0.9 V, the films were Se-rich, and at potentials higher than -1.1 V, the films were In-rich.

Pern *et al.*⁶³⁾ achieved the fabrication of polycrystalline thin films of CuInSe_2 on molybdenum-coated alumina substrates via a simple one-step electrodeposition. The composition of the electrodeposited thin films showed a slight dependence on the deposition potential. As the potential decreased from -0.55 V to -0.75 V vs. SCE, the indium content gradually increased.

In the potentiostatic deposition of CuInSe films performed by Ueno *et al.*,⁶⁴⁾ it was observed that (i) a CuInSe_2 film with a composition close to the stoichiometric ratio was exclusively deposited at -0.8 V vs. SCE, (ii) a positive shift in the potential was responsible for the codeposition of the Cu_3Se_2 phase, and (iii) a negative shift led to contamination by metallic indium.

Guillén and Herrero^{65,66)} reported that the composition of electrodeposited CuInSe_2 thin film was strongly determined by the applied deposition potential. As the deposition potential became more anodic, the copper and selenium content increased. With greater film thickness, the film composition became uniform and the Cu/In ratio approached 1. Films prepared at -0.6 V vs. SCE showed a direct optical transition, and the measured band gap energy was 0.99 ± 0.22 eV.

The preparation of CI(G)S is usually carried out

under acidic condition less than pH 2, however several studies with uses of complex agents have been carried out at the pH higher than 4. The potentiostatic deposition of a CuInSe_2 system was investigated by Ganchev *et al.*⁶¹⁾ The electrodeposition was carried out in a 4 M KSCN solution in a potential range of -0.7 V to -1 V vs. SCE. CuInSe_2 thin films deposited at -0.8 V had the closest stoichiometric composition. In a pH range of 4-5, the deposition rate decreased sharply but the obtained films were smooth, dense, and homogeneous. Arauzo *et al.*⁸⁹⁾ performed electrochemical growth of CuInSe_2 films in alkaline medium of pH 8.5. To avoid the formation of elemental Cu and In, diethylenetriamine was used as a complexing agent. The use of diethylenetriamine brought the copper reduction potential near the deposition potential of indium. The analysis of the films revealed the stoichiometric formula $\text{Cu}_{2.40}\text{In}_{1.00}\text{Se}_{3.40}$ with an excess of CuSe and an additional phase attributed to In_2O_3 was also detected.

Bhattacharya *et al.*⁵²⁾ obtained electron microprobe analysis (EMPA) data of as-deposited CuInSe layers prepared at different potentials. At potentials of -0.5 , -0.55 , -0.6 , and -0.65 V vs. SCE, the film compositions were $\text{Cu}_{1.17}\text{In}_{0.89}\text{Se}_2$, $\text{Cu}_{1.21}\text{In}_{0.90}\text{Se}_2$, $\text{Cu}_{1.31}\text{In}_{0.86}\text{Se}_2$, and $\text{Cu}_{1.16}\text{In}_{0.95}\text{Se}_2$, respectively.

Gujar *et al.*¹⁵³⁾ prepared CuInSe_2 thin films by electrodeposition at constant potentials from -600 to -1000 mV vs. Ag/AgCl for 20 min without stirring. The CuInSe_2 films deposited at a lower deposition potential were found to possess a well-defined compact dendrite structure with a size of ~ 400 nm, while higher cathodic potentials beyond -700 mV led to porous deposits. The Cu/In/Se ratio of the electrodeposited CuInSe_2 thin films was determined to be near 1:1:2 at -700 mV vs. Ag/AgCl.

Chassaing *et al.*⁹¹⁾ carried out one-step electrodeposition of CuInSe_2 potentiostatically. With an applied potential of -0.9 V vs. MSE, the Se/Cu ratio was 1.9 and the In/Cu ratio was 0.9.

The deposition of CuInSe_2 layers onto CdS layers was carried out potentiostatically⁸⁴⁾. The applied deposition potential was varied between -1.10 and -1.00 V vs. MSE. Variations of the deposition potential within 0.1 V changed the defect structure of the CIS layers and influenced the interdiffusion of cadmium and sulfur from the CdS window into the CIS absorber layer.

CuInGaSe_2 nanowires were electrodeposited potentiostatically into AAMs (anodic alumina membrane) from aqueous solutions containing Cu^{2+} , In^{3+} , Ga^{3+} ,

and Se^{4+} at room temperature for 1 h.¹⁰⁵⁾ Electrodeposition was performed at a constant potential varying from -0.605 V to -1.05 V vs. NHE. The deposited film, whose composition of $\text{Cu}_{0.203}\text{In}_{0.153}\text{Ga}_{0.131}\text{Se}_{0.513}$ is quite close to the stoichiometric composition, was formed at -0.905 V vs. NHE. These nanowires displayed a cathodic photocurrent and an optical band gap of 1.55 eV.

Sahu *et al.*¹³¹⁾ reported that reproducible and stoichiometric CuInSe_2 films were obtained at a constant current density of 6 mA cm^{-2} . The color of the deposit obtained at that current density was black, while the colors obtained at a higher and lower current density were white and blue, and brown, respectively.

Garg *et al.*¹³³⁾ studied the formation of thin films of copper indium sulfoselenide ($\text{CuInS}_x\text{Se}_{2-x}$) using the galvanostatic deposition technique. The pH level of the bath solution was greater than 9. It was observed that an increase in the current density to more than 1.4 mA cm^{-2} or a concentration of sodium thiosulfate above 0.4 mM (chalcogen atomic ratio S/Se 0.25) resulted into less adherent and powdery films.

The codeposition of $\text{CuIn}_{1-x}\text{Ga}_x\text{Se}_2$ on Mo glass was performed by Fu *et al.*¹⁰³⁾ They investigated the electrochemical kinetic behavior of each ion at the metal-solution interface, using electrochemical impedance spectroscopy (EIS). The electrodeposition of $\text{CuIn}_{1-x}\text{Ga}_x\text{Se}_2$ was strongly influenced by the structure of the electrical double layer existing between the substrate and the electrolyte with different concentrations of Ga^{3+} . With an increase in the electrodeposition time, the kinetic behavior of this deposition system was gradually dominated by the diffusion process, rather than the charge-transfer process. They concluded that the electrodeposition time and the concentration of Ga^{3+} were the main parameters governing the growth of the CIGS thin film by electrodeposition.

The antimony content of InSb alloy deposited from citrate complexes of antimony and indium increased with an increase in temperature at constant currents of $1\text{--}4$ A/dm^2 . In this current density range, the brightness of the deposits depended on the temperature and the solution pH.¹²⁷⁾

Fernández Valverde *et al.*⁸¹⁻⁸³⁾ prepared thin films of p-CuInSe₂ that were modified with selenium and ruthenium (CuInSe_x and $\text{CuInSe}_x\text{Ru}_y$). These modified films induced an excess surface charge that enhanced the cathodic photocurrent in a sulfuric acid solution. The increased photocurrent of both Se- and Ru- modi-

fied CuInSe_2 films was attributed to the hydrogen evolution reaction and also to a photodegradation process.⁸²⁾ The Ru films deposited on the CuInSe_2 prevented semiconductor corrosion in acidic media and enhanced the photoelectrochemical response.⁸³⁾

8. Conclusions and Outlook

Many researchers have fabricated indium alloys by means of one-step potentiostatic deposition. In this case, it is very important to control the deposition parameters, such as the bath composition, the deposition potential or current density, the pH of the bath solution, and post-treatment due to their influence on the film's properties and quality. The composition of an alloy thin film strongly depends on the deposition potential (or current) and the composition of the bath. In the preparation of indium alloys, as the cathodic deposition potential increased in a negative direction or as the current density increased, the percentage of indium in the deposit increased, because indium generally was not nobler than the other metals in the deposit alloys. The addition of a complexing agent shifted the metal deposition potential in a more negative direction. Thermal treatment has also been found to influence the alloy structure, surface morphology, and properties of alloys. Efficient electrodeposition conditions for the formation of alloys that contain indium have yet to be developed for the successful realization of indium-containing materials, especially for CIGS solar cells. The summaries of the data presented in the nine tables in this article may be helpful in designing the desired experimental conditions to prepare a targeted alloy that contains indium.

Acknowledgements

This work was financially supported by National Research Foundation of Korea (2010-0029164).

References

1. A. M. Alfantazi and R. R. Moskalyk, *Minerals Engineering*, **16**, 687 (2003).
2. J. R. Mills, R. A. King and C. E. T. White "Indium," C.A. Hampel (ed.), *Rare metals handbook*, Chapman and Hall Ltd, London, p. 220 (1961).
3. J. R. Mills, B. G. Hunt and G. H. Turner, *J. Electrochem. Soc.*, **100**, 136 (1953).
4. C. J. Smithells, W. F. Gale and T. C. Totemeier (eds.),

- Smithells metals reference book*, 8th ed. Elsevier Butterworth-Heinemann, Amsterdam, II-354 (2004).
5. R. Piercy and N. A. Hampson, *J. Appl. Electrochem.*, **5**, 1 (1975).
 6. V. V. Losev and A. I. Molodov "Indium," A.F. Bard (ed.), *Encyclopedia of electrochemistry of the elements*, vol. 6, Marcel Dekker Inc, New York, p. 1 (1976).
 7. Y. Chung and C.W. Lee, *J. Electrochem. Sci. Tech.*, **3**, 1 (2012).
 8. F. C. Walsh and D. R. Gabe, *Surface Tech.*, **13**, 304 (1981).
 9. R. K. Pandey, S.N. Sahu and S. Chandra, *Handbook of semiconductor electrodeposition*, Marcel Dekker, Inc., New York, (1996).
 10. S. Ozer and C. Besikci, *J. Phys. D: Appl. Phys.*, **36**, 559 (2003).
 11. C. S. Johnson, J. T. Vaughey, M. M. Thackeray, T. Sarakonsri, S. A. Hackney, L. Fransson, K. Edström and J.O. Thomas, *Electrochem. Comm.*, **2**, 595 (2000).
 12. Y. Yang, L. Li, X. Huang, G. Li and L. Zhang, *J. Mater. Sci.*, **42**, 2753 (2007).
 13. S. Y. Wang, S. H. Lin and Y. M. Houg, *Appl. Phys. Lett.*, **51**, 83 (1987).
 14. T. S. Chao, C. L. Lee and T. F. Lei, *J. Mater. Sci. Lett.*, **12**, 721(1993).
 15. T. Inushima, V. V. Mamutin, V. A. Vekshin, S. V. Ivanov, T. Sakon, M. Motokawa, and S. Ohoya, *J. Crystal Growth*, **227-228**, 481 (2001).
 16. T. P. Pearsall and M. Papuchon, *Appl. Phys. Lett.*, **33**, 640 (1978).
 17. W. J. Li, Y. N. Zhou and Z. W. Fu, *Appl. Surf. Sci.*, **257**, 2881 (2011).
 18. V. A. Williams, *J. Electrochem. Soc.*, **113**, 234 (1966).
 19. V. S. Saji, S. M. Lee and C.W. Lee, *J. Korean Electrochem. Soc.*, **14**, 61 (2011).
 20. V. S. Saji, I. H. Choi and C. W. Lee, *Solar Energy*, **85**, 2666 (2011).
 21. J. L. Vossen and E.S. Poliniak, *Thin Solid Films*, **13**, 281(1972).
 22. L. L. Kazmerski, M. S. Ayyagari and G. A. Sanborn, *J. Appl. Phys.*, **46**, 4865 (1975).
 23. A. Yamamoto, M. Tsujino, M. Ohkubo and A. Hashimoto, *Sol. Energ. Mater. Sol. Cells*, **35**, 53 (1994).
 24. G. S. Anderson and G.K. Wehner, *Surf. Sci.*, **2**, 367 (1964).
 25. J. Szczyrbowski, A. Czapla and M. Jachimowski, *Thin Solid Films*, **42**, 193 (1977).
 26. R. Venkataraghavan, K. M. Satyalakshmi, K. S. R. K. Rao, A. K. Sreedhar, M. S. Hegde and H. L. Bhat, *Bull. Mater. Sci.*, **19**, 123 (1996).
 27. T. Saitoh, S. Matsubara and S. Minagawa, *J. Electrochem. Soc.*, **123**, 403 (1976).
 28. J. Kane, H. P. Schweizer and W. Kern, *Thin Solid Films*, **29**, 155 (1975).
 29. R. N. Bhattacharya, *J. Electrochem. Soc.*, **130**, 2040 (1983).
 30. C. W. Bates, K. F. Nelson, S. A. Raza, J. B. Mooney, J. M. Recktenwald, L. Macintosh and R. Lamoreaux, *Thin Solid Films*, **88**, 279 (1982).
 31. C. R. Abernathy, C. W. Bates, A. A. Anani, B. Haba and G. Smedstad, *Appl. Phys. Lett.*, **45**, 890 (1984).
 32. S. A. Ringel, A. W. Smith, M. H. MacDougall and A. Rohatgi, *J. Appl. Phys.*, **70**, 881 (1991).
 33. M. Kawaji, S. Baba and A. Kinbara, *Thin Solid Films*, **58**, 183 (1979).
 34. A. Brenner, "Electrodeposition of Alloys," 2 volumes, Academic press, New York (1963).
 35. D. Lincot, J. F. Guillemoles, S. Taunier, D. Guimard, J. Sixx-Kurdi, A. Chaumont, O. Roussel, O. Ramdani, C. Hubert, J.P. Fauvarque, N. Bodereau, L. Parissi, P. Panheleux, P. Fanouillere, N. Naghavi, P. P. Grand, M. Benfarah, P. Mogensen and O. Kerrec, *Solar Energy*, **77**, 725 (2004).
 36. O. G. Zarubitskii, A. A. Omel'chuk, V. G. Budnik and V. T. Melekhin, *Russ. J. Appl. Chem.*, **75**, 1965 (2002).
 37. D. R. Lide (ed), *CRC Handbook of Chemistry and Physics*, 88th ed. CRC Press, Boca Raton, FL, p. 8 (2008).
 38. J. W. Cuthbertson, N. Parkinson and H. P. Rooksby, *J. Electrochem. Soc.*, **100**, 107 (1953).
 39. F. A. Kröger, *J. Electrochem. Soc.*, **125**, 2028 (1978).
 40. R. N. Bhattacharya, D. Cahen and G. Hodes, *Solar Energy Mater.*, **10**, 41 (1984).
 41. J. Ortega and J. Herrero, *J. Electrochem. Soc.*, **136**, 3388 (1989).
 42. S. N. Vinogradov, Y. P. Perelygin and E. A. Efimov, *Soviet Electrochem.*, **23**, 909 (1987).
 43. S. B. Saidman, A. G. Munoz and J. B. Bessone, *J. Appl. Electrochem.*, **29**, 245 (1999).
 44. A. G. Munoz, S. B. Saidman and J. B. Bessone, *J. Appl. Electrochem.*, **29**, 1297 (1999).
 45. E. Dalchiele, S. Cattarin, M. Musiani, U. Casellato, P. Guerriero and G. Rossetto, *J. Electroanal. Chem.*, **418**, 83 (1996).
 46. J. J. McChesney, J. Haigh, I. M. Dharmadasa and D. J. Mowthorpe, *Optical Materials*, **6**, 63 (1996).
 47. T. Fulop, C. Bekele, U. Landau, J. Angus and K. Kash, *Thin Solid Films*, **449**, 1 (2004).
 48. M. I. Khan, X. Wang, K. N. Bozhilov and C. S. Ozkan, *J. Nanomaterials*, **2008**, 698759 (2008).
 49. C. Sanjeeviraja and T. Mahalingam, *J. Mater. Sci. Lett.*, **11**, 525 (1992).
 50. Y. Igasaki and T. Fufiwara, *J. Crystal Growth*, **158**, 268 (1996).
 51. S. Massaccesi, S. Sanchez and J. Vedel, *J. Electroanal. Chem.*, **412**, 95 (1996).
 52. R. N. Bhattacharya, A. M. Fernandez, M. A. Contreras, J. Keane, A. L. Tennant, K. Ramanathan, J. R. Tuttle, R. N. Noufi and A.M. Hermann, *J. Electrochem. Soc.*, **143**, 854 (1996).
 53. A. Kampmann, V. Sittinger, J. Rechid and R. Reineke-Koch, *Thin Solid Films*, **361-362**, 309 (2000).
 54. S. Gopal, C. Viswanathan, M. Thamilselvan, K. Premnazeer, S. K. Narayandass and D. Mangalaraj, *Ionics*, **10**, 300 (2004).

55. S. Gopal, C. Viswanathan, B. Karunakaran, S. K. Narayandas, D. Mangalaraj, and Y. Yi, *Cryst. Res. Technol.*, **40**, 557 (2005).
56. G. Hodes, T. Engelhard, D. Cahen, L. Lawrence, L. L. Kazmerski and C.R. Herrington, *Thin Solid Films*, **128**, 93 (1985).
57. D. Pottier and G. Maurin, *J. Appl. Electrochem.*, **19**, 361 (1989).
58. P. P. Prosini, M. L. Addonizio, A. Antonaia and S. Loreti, *Thin Solid Films*, **288**, 90 (1996).
59. S. Nakamura and A. Yamamoto, *Sol. Energ. Mater. Sol. Cells*, **75**, 81 (2003).
60. R. N. Bhattacharya and K. Rajeshwar, *Solar Cells*, **16**, 237 (1986).
61. M. G. Ganchev and K. D. Kochev, *Sol. Energ. Mater. Sol. Cells*, **31**, 163 (1993).
62. E. Tzvetkova, N. Stratieva, M. Ganchev, I. Tomov, K. Ivanova and K. Kochev, *Thin Solid Films*, **311**, 101 (1997).
63. F. J. Pern, J. Goral, R. J. Matson, T. A. Gessert and R. Noufi, *Solar Cells*, **24**, 81 (1988).
64. Y. Ueno, H. Kawai, T. Sugiura and H. Minoura, *Thin Solid Films*, **157**, 159 (1988).
65. C. Guillén and J. Herrero, *Solar Energy Mater.*, **23**, 31 (1991).
66. C. Guillén and J. Herrero, *Thin Solid Films*, **195**, 137 (1991).
67. C. Guillén and J. Herrero, *J. Electrochem. Soc.*, **141**, 225 (1994).
68. C. Guillén and J. Herrero, *J. Electrochem. Soc.*, **142**, 1834 (1995).
69. C. Guillén and J. Herrero, *Sol. Energ. Mater. Sol. Cells*, **43**, 47 (1996).
70. Y. Sudo, S. Endo and T. Irie, *Jpn. J. Appl. Phys.*, **32**, 1562 (1993).
71. L. Thouin, S. Massaccesi, S. Sanchez and J. Vedel, *J. Electroanal. Chem.*, **374**, 81 (1994).
72. D. Guimard, P. P. Grand, N. Bodereau, P. Cowache, J. F. Guillemoles, D. Lincot, S. Taunier, M. Ben Farah, P. Mogensen and O. Kerrec, *29th IEEE Photovoltaic Specialists Conference*, 692 (2002).
73. L. Thouin and J. Vedel, *J. Electrochem. Soc.*, **142**, 2996 (1995).
74. J. F. Guillemoles, A. Lusson, P. Cowache, S. Massaccesi, J. Vedel and D. Lincot, *Adv. Mater.*, **6**, 376 (1994).
75. J. F. Guillemoles, P. Cowache, S. Massaccesi, L. Thouin, S. Sanchez, D. Lincot and J. Vedel, *Adv. Mater.*, **6**, 379 (1994).
76. J. F. Guillemoles, P. Cowache, A. Lusson, K. Fezzaa, F. Boisvion, J. Vedel and D. Lincot, *J. Appl. Phys.*, **79**, 7293 (1996).
77. J. Vedel, L. Thouin and D. Lincot, *J. Electrochem. Soc.*, **143**, 2173 (1996).
78. A. M. Fernandez, P. J. Sebastian, R. N. Bhattacharya, R. N. Noufi, M. A. Contreras and A.M. Hermann, *Semicond. Sci. Tech.*, **11**, 964 (1996).
79. M. E. Calixto, P. J. Sebastian, R. N. Bhattacharya and R.N. Noufi, *Sol. Energ. Mater. Sol. Cells*, **59**, 75 (1999).
80. O. Solorza-Feria and R. Rivera Noriega, *J. Mater. Sci.*, **30**, 2616 (1995).
81. E. Ordoñez Regil, S. M. Fernández-Valverde, R. Rivera Noriega and O. Solorza-Feria, *J. Mater. Sci.*, **31**, 5347 (1996).
82. S. M. Fernández-Valverde, E. Ordoñez Regil, R. Valencia Alvarado, R. Rivera Noriega and O. Solorza-Feria, *Int. J. Hydrogen Energy*, **22**, 581 (1997).
83. A. López Alanis, J. R. Vargas García, R. Rivera and S. M. Fernández Valverde, *Int. J. Hydrogen Energy*, **27**, 143 (2002).
84. A. Kampmann, P. Cowache, D. Lincot and J. Vedel, *J. Electrochem. Soc.*, **146**, 150 (1999).
85. R. Ugarte, R. Schrebler, R. Córdova, E. A. Dalchiele and H. Gómez, *Thin Solid Films*, **340**, 117 (1999).
86. K. T. L. De Silva, W. A. A. Priyantha, J. K. D. S. Jayanetti, B. D. Chithrani, W. Siripala, K. Blake and I. M. Dharmadasa, *Thin Solid Films*, **382**, 158 (2001).
87. F. Chraïbi, M. Fahoume, A. Ennaoui and J. L. Delplancke, *Phys. Stat. Sol. (a)*, **186**, 373 (2001).
88. L. Zhang, F. D. Jiang and J. Y. Feng, *Sol. Energ. Mater. Sol. Cells*, **80**, 483 (2003).
89. J. Araujo, R. Ortíz, A. López-Rivera, J. M. Ortega, M. Montilla and D. Alarcón, *J. Solid State Electrochem.*, **11**, 407 (2007).
90. A. Ihlal, K. Bouabid, D. Soubane, M. Nya, O. Ait-Taleb-Ali, Y. Amira, A. Outzourhit and G. Nouet, *Thin Solid Films*, **515**, 5852 (2007).
91. E. Chassaing, P. P. Grand, O. Ramdani, J. Vigneron, A. Etcheberry and D. Lincot, *J. Electrochem. Soc.*, **157**, D387 (2010).
92. T. Yukawa, K. Kuwabara and K. Koumoto, *Thin Solid Films*, **286**, 151 (1996).
93. S. Nakamura and A. Yamamoto, *Sol. Energ. Mater. Sol. Cells*, **49**, 415 (1997).
94. T. Yukawa, K. Kuwabara and K. Koumoto, *Thin Solid Films*, **280**, 160 (1996).
95. T. Ishizaki, N. Saito and A. Fuwa, *Surf. Coat. Tech.*, **182**, 156 (2004).
96. G. Mengoli, M. M. Musiani and F. Paolucci, *J. Electroanal. Chem.*, **332**, 199 (1992).
97. L. Ribeaucourt, G. Savidand, D. Lincot and E. Chassaing, *Electrochim. Acta*, **56**, 6628 (2011).
98. R. N. Bhattacharya, W. Batchelor, J. F. Hiltner and J. R. Sites, *Appl. Phys. Lett.*, **75**, 1431 (1999).
99. R. N. Bhattacharya, J. F. Hiltner, W. Batchelor, M. A. Contreras, R. N. Noufi and J. R. Sites, *Thin Solid Films*, **361–362**, 396 (2000).
100. R.N. Bhattacharya and A.M. Fernandez, *Sol. Energ. Mater. Sol. Cells*, **76**, 331 (2003).
101. R. N. Bhattacharya, *J. Electrochem. Soc.*, **157**, D406 (2010).
102. P. J. Sebastian, M. E. Calixto, R. N. Bhattacharya and

- R. Noufi, *Sol. Energ. Mater. Sol. Cells*, **59**, 125 (1999).
103. Y. P. Fu, R. W. You and K. K. Lew, *J. Electrochem. Soc.*, **156**, E133 (2009).
104. Y. Lai, F. Liu, S. Kuang, J. Liu, Z. Zhang, J. Li and Y. Liu, *Electrochem. Solid-State Lett.*, **12**, D65 (2009).
105. R. Inguanta, P. Livreri, S. Piazza and C. Sunseri, *Electrochem. Solid-State Lett.*, **13**, K22 (2010).
106. R. Diaz, G. San Vicente, J. M. Merino, F. Rueda, P. Ocon and P. Herrasti, *J. Mater. Chem.*, **10**, 1623 (2000).
107. G. Mengoli, M. M. Musiani, F. Paolucci and M. Gazzano, *J. Appl. Electrochem.*, **21**, 863 (1991).
108. F. Paolucci, G. Mengoli and M.M. Musiani, *J. Appl. Electrochem.*, **20**, 868 (1990).
109. N. R. de Tacconi and K. Rajeshwar, *J. Electroanal. Chem.*, **444**, 7 (1998).
110. J. Herrero and J. Ortega, *Solar Energy Mater.*, **16**, 477 (1987).
111. T. L. Wade, L. C. Ward, C. B. Maddox, U. Happek and J.L. Stickney, *Electrochem. Solid-State Lett.*, **2**, 616 (1999).
112. T. L. Wade, R. Vaidyanathan, U. Happek and J. L. Stickney, *J. Electroanal. Chem.*, **500**, 322 (2001).
113. R. P. Raffaele, J. G. Mantovani, R. Friedfeld, S. G. Bailey and S. M. Hubbard, *Proceedings of the 26th IEEE PVSC*, 559 (1997).
114. C. Guillén and J. Herrero, *J. Electrochem. Soc.*, **143**, 493 (1996).
115. J. Herrero and J. Ortega, *Solar Energy Mater.*, **20**, 53 (1990).
116. T. P. Gujar, V. R. Shinde, J. W. Park, H.K. Lee, K.D. Jung, and O.S. Joo, *J. Electrochem. Soc.*, **155**, E131 (2008).
117. R. Friedfeld, R. P. Raffaele and J. G. Mantovani, *Sol. Energ. Mater. Sol. Cells*, **58**, 375 (1999).
118. J. Herrero and J. Ortega, *Solar Energy Mater.*, **17**, 357 (1988).
119. S. Cattarin, M. Musiani, U. Casellato, G. Rossetto, G. Razzini, F. Decker, and B. Scrosati, *J. Electrochem. Soc.*, **142**, 1267 (1995).
120. T. S. Dobrovolska, L. Veleva, I. Krastev and A. Zielonka, *J. Electrochem. Soc.*, **152**, C137 (2005).
121. T. S. Dobrovolska, I. Krastev and A. Zielonka, *J. Appl. Electrochem.*, **35**, 1245 (2005).
122. G. A. Peristaya and Y. P. Perelygin, *Russ. J. Appl. Chem.*, **72**, 1220 (1999).
123. G. A. Peristaya and Y. P. Perelygin, *Protection of Metals*, **36**, 294 (2000).
124. Y. N. Sadana, *Surf. Tech.*, **6**, 369 (1978).
125. Y. P. Perelygin, Y. N. Kirilina and A.S Meshcheryakov, *Russ. J. Appl. Chem.*, **83**, 165 (2010).
126. S. N. Sahu, *J. Mater. Sci. Lett.*, **8**, 533 (1989).
127. Y. N. Sadana and J. P. Singh, *Plating and Surface Finishing*, **72**, 64 (1985).
128. Y. N. Sadana and Z. Z. Wang, *Surf. Tech.*, **25**, 17 (1985).
129. S. Aksu, J. Wang, and B.M. Basol, *Electrochem. Solid-State Lett.*, **12**, D33 (2009).
130. T. Ishizaki, N. Saito and A. Fuwa, *Materials Transactions JIM*, **40**, 867 (1999).
131. S. N. Sahu, R. D. L. Kristensen and D. Haneman, *Solar Energy Mater.*, **18**, 385 (1989).
132. K. K. Mishra and K. Rajeshwar, *J. Electroanal. Chem.*, **271**, 279 (1989).
133. P. Garg, A. Garg and J.C. Garg, *Thin Solid Films*, **206**, 236 (1991).
134. T. L. Chu, S. S. Chu, S. C. Lin and J. Yue, *J. Electrochem. Soc.*, **131**, 2182 (1984).
135. Q. Huang, K. Reuter, S. Amhed, L. Deliglanni, L. T. Romankiw, S. Jaime, P. P. Grand and V. Charrier, *J. Electrochem. Soc.*, **158**, D57 (2011).
136. Q. Huang, B. C. Baker-O'Neal, J. J. Kelly, P. Broekmann, A. Wirth, C. Emnet, M. Martin, M. Hahn, A. Wagner and D. Mayer, *Electrochem. Solid-State Lett.*, **12**, D27 (2009).
137. V. M. Kozlov, V. Agrigento, G. Mussati and L.P. Bicelli, *J. Alloys Compd.*, **288**, 255 (1999).
138. V. K. Kapur, B. M. Basol and E. S. Tseng, *Solar Cells*, **21**, 65 (1987).
139. R. N. Bhattacharya, M. K. Oh and Y. Kim, *Sol. Energ. Mater. Sol. Cells*, **98**, 198 (2012).
140. V. M. Kozlov, V. Agrigento, D. Bontempi, S. Canegallo, C. Moraitou, A. Toussimi, L.P. Bicelli and G. Serravalle, *J. Alloys Compd.*, **259**, 234 (1997).
141. S. Canegallo, V. Demeneopoulos, L. P. Bicelli and G. Serravalle, *J. Alloy Compd.*, **216**, 149 (1994).
142. S. Canegallo, V. Demeneopoulos, L. P. Bicelli and G. Serravalle, *J. Alloy Compd.*, **228**, 23 (1995).
143. S. Canegallo, V. Agrigento, C. Moraitou, A. Toussimi, L. P. Bicelli and G. Serravalle, *J. Alloy Compd.*, **234**, 211 (1996).
144. S. M. Rabchynski, D. K. Ivanou and E.A. Streltsov, *Electrochem. Comm.*, **6**, 1051 (2004).
145. C.H. Sonu and T.J. O'Keefe, *Mater. Charact.*, **33**, 311 (1994).
146. F. Liu, C. Huang, Y. Lai, A. Zhang, J. Li and Y. Liu, *J. Alloys Compd.*, **509**, L129 (2011).
147. S. Phok, S. Rajaputra and V.P. Singh, *Nanotechnology*, **18**, 475601 (2007).
148. M. Kemell, M. Ritala, H. Saloniemi, M. Leskelä, T. Sajavaara and E. Rauhala, *J. Electrochem. Soc.*, **147**, 1080 (2000).
149. M. Kemell, H. Saloniemi, M. Ritala and M. Leskelä, *J. Electrochem. Soc.*, **148**, C110 (2001).
150. M. Kemell, M. Ritala and M. Leskelä, *J. Mater. Chem.*, **11**, 668 (2001).
151. T. J. Whang, M. T. Hsieh, Y. C. Kao and S.J. Lee, *Appl. Surf. Sci.*, **255**, 4600 (2009).
152. T. J. Whang, M. T. Hsieh, Y. C. Kao and S. J. Lee, *Appl. Surf. Sci.*, **257**, 1457 (2010).
153. T. P. Gujar, V. R. Shinde, J. W. Park, H. K. Lee, K. D. Jung and O.S. Joo, *J. Electrochem. Soc.*, **156**, E8 (2009).
154. T. S. Dobrovolska, I. Krastev and A. Zielonka, *Russ. J. Electrochem.*, **44**, 676 (2008).